Assessing the opportunity to produce Nitinol medical device components using additive manufacturing

by

Arvind R. Kalidindi

Ph.D. Materials Science and Engineering
Massachusetts Institute of Technology, 2018

SUBMITTED TO THE DEPARTMENT OF MATERIALS SCIENCE AND ENGINEERING IN PARTIAL FULFILLMENT OF THE REQUIREMENTS OF THE DEGREE OF

Master of Business Administration

at the

MASSACHUSETTS INSTITUTE OF TECHNOLOGY

March 2019

Signature of Author: Signature redacted
.....
Sloan School of Management
March 01, 2019

Certified by: Signature redacted
.....
Thomas Roemer
Senior Lecturer, Operations Management
Thesis Supervisor

Signature redacted
.....
Christopher A. Schuh
Danae and Vasilis Salapatas Professor of Metallurgy
Thesis Supervisor

Accepted by: Signature redacted
.....
Maura Henson
Assistant Dean, MBA Program
MIT Sloan School of Management

Assessing the opportunity to produce Nitinol medical device components using additive manufacturing

by

Arvind R. Kalidindi

Submitted to the Sloan School of Management

on March 01, 2019 in Partial Fulfillment of the Requirements for the

Degree of Master of Business Administration

ABSTRACT

Nitinol is an important alloy for medical device applications due to its exceptional combination of strength and elasticity. Most Nitinol is produced in wire form and then braided or laser cut into the complex geometries needed for medical device applications. These manufacturing processes are costly and can be labor-intensive. Additive manufacturing, or 3D printing, offers a tantalizing alternative to the status quo of Nitinol manufacturing as the desired part can be printed to shape, greatly simplifying the operations and cost of producing medical device components.

Working with Boston Scientific in Clonmel, Ireland, roughly 100 Nitinol samples were additively manufactured to determine whether quality parts could be printed. Through a design of experiment procedure, the 3D printing parameters were optimized to develop settings for parts with high relative density, low internal defects, and low impurity concentrations, meeting the ASTM F2063 standards for medical device-grade Nitinol. The main challenge from an engineering perspective is the loss of Ni during printing, which could require either higher power lasers or sourcing high Ni content powder to reach the desired properties. Operationally, a cost accounting model was developed to match the expected operational setup for additively manufacturing Nitinol, with smaller components comparing favorably cost-wise to traditionally manufactured Nitinol components. The engineering and business analyses were combined to determine the best applications considering Nitinol properties used (superelasticity, shape memory, and ductility) and the opportunity for 3D printing (prototyping, replacing existing Nitinol parts, developing new Nitinol parts). The best opportunities in the short-term for this technology were identified to be prototyping and developing new Nitinol components targeting ductility and shape memory Nitinol applications.

Table of Contents

List of Figures

List of Tables

Acknowledgements

First and foremost, I would like to thank Michael Keane, Kevin O'Riordan, and Rob Hannon for hosting me at Boston Scientific in Clonmel and giving me the opportunity to work on this exciting project. I also want to thank Steve Schiveley for reaching out with this opportunity. The six months that I spent in Clonmel were a great learning experience for me and felt incredibly special. This work would not be possible without the additive team: Rob, James, Mark, Aine, Liam, Stephen, Conor, and Lauren – thank you for welcoming me to the team and for your friendship.

I also want to thank the LGO program for making this project possible. Patty and Thomas, thank you for taking a chance on integrating me into the LGO program. I'm forever grateful for having the opportunity to be a part of LGO! Thomas, thank you for being a terrific advisor for this project; your visits to Ireland were immensely helpful in getting outside perspective and shaping the project into this complete thesis. I also want to thank my 48 classmates for their support and for helping me navigate business school (and thanks Megan, Ken, and Kristin for organizing a nice respite to Northern Ireland during the internship!). This project would never have happened had my Ph.D advisor not been Chris Schuh. Chris – thank you for giving me permission to explore this opportunity and for advising this project.

Finally, I want to thank my friends and family for their love, support, and encouragement. Neha, thank you for supporting my choice to go overseas for this work and being a wonderful partner through this process. And to my mother, Manju, my father, Surya, and my brother, Bharath, I'm incredibly grateful to have you all constantly support me and give me excellent advice when deciding to take on new projects such as this.

1. Introduction

Additive manufacturing is a rapidly growing method for making components directly into their final shape from feedstock. Synonymous with 3D printing, additive manufacturing enables parts to be processed to shape by adding material layer by layer compared to traditional 'subtractive' manufacturing methods which start with a larger piece of raw material and cut out the desired part shape (e.g. milling or laser cutting). Additive manufacturing offers advantages in reducing the cost of complex designs and low volume components compared to traditional manufacturing methods [1-4].

While additive manufacturing originally gained traction as a way to prototype and build plastic parts, the variety of materials for which high quality additively manufactured components can be developed has grown in the past decade, with a large increase in suppliers of additive manufacturing printers particularly for metallic materials [4]. The growth of metal additive manufacturing has been enabled by the ability of engineers to achieve good structural properties in printed parts, which include reducing the amount and size of critical defects (such as pores) and controlling the chemistry to minimize the presence of impurities which can embrittle the alloy [5-7]. The ability to create high quality, complex, low volume components has made metal additive manufacturing an important technology in several industries using a number of different additive manufacturing technologies as required by the different scale of parts and different mechanical property requirements [3, 4].

This thesis explores the opportunity to use metal additive manufacturing in the medical device industry to produce a special alloy known as Nitinol, which is an equiatomic alloy of Nickel (Ni) and Titanium (Ti) with the chemical notation NiTi. Nitinol has incredible elasticity, termed superelasticity, enabled by a solid-state phase transformation under stress. To achieve superelasticity requires precise control over chemistry and microstructure, which makes 3D printing Nitinol a complex engineering challenge. In addition, as most Nitinol parts in the medical device industry have been designed to accommodate the availability of Nitinol as a wire or tube, the advantages of additive manufacturing need to be analyzed in an operational context to understand where the best use cases for this technology lie (i.e. prototyping, commercial, or new products) and which Nitinol properties are most practical to design around (superelasticity, shape

memory, and/or high ductility). In this thesis, the feasibility of using metal additive manufacturing, in particular selective laser sintering, to produce Nitinol components is assessed both from an engineering and operational perspective to develop insight into the potential opportunities of this technology in the medical device industry and the major challenges that need to be overcome.

1.1. Nitinol: Properties, Applications, and Current Industry Challenges

1.1.1 Superelastic and Shape Memory properties of Nitinol

Nitinol, or NiTi, is a metallic compound formed by alloying Ni and Ti together at around equiatomic compositon (i.e. 50 at.% Ni and 50 at.% Ti). This compound can exist at equilibrium with two crystalline phases, which are termed the martensite and austenite phases. The unique properties of Nitinol are a result of phase transitions between the martensite and austenite phases using either heat or mechanical stress.

Superelasticity describes the large elongations and compressions (known as 'strains' in mechanics) that Nitinol can endure elastically, i.e. with minimal permanent deformation. Superelasticity occurs when Nitinol is in the austenite phase. As Nitinol undergoes deformation under a force (more generally called a 'stress'), it can transform into martensite which leads to further deformation. When the force is released, the martensite transforms back to austenite and recovers to its original shape. Because of the transformation from austenite to martensite, Nitinol can have elastic elongations of 10-20 times that of stainless steel [8] with strains greater than 10% (which means a 10% extension or compression from the undeformed state). Figure 1 schematically shows a typical mechanical testing curve, known as a stress-strain curve, for Nitinol that exhibits superelasticity (Figure 1). Superelasticity is a valuable mechanical property in Nitinol: it allows Nitinol to have a reasonably high strength as a metal while having an elasticity/bendability closer to that of a plastic, which makes it useful in medical device applications where a combination of strength and elasticity are required as well as for deploying certain devices which can be compressed into a small tube and decompress into their original shape when pushed into the body [9].

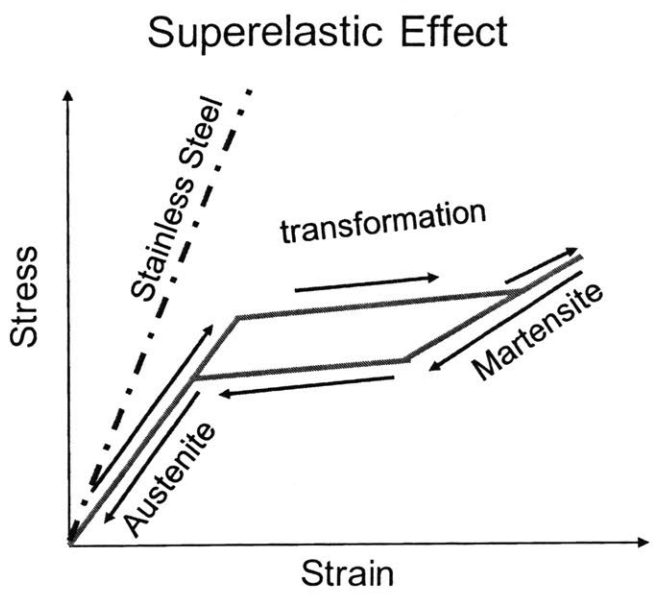

Figure 1. A schematic showing the superelastic effect for Nitinol where a transformation from austenite to martensite leads to significantly larger (10-20x) elastic deformation than conventional metal alloys.

The shape memory effect is similarly a result of the transformation between austenite and martensite, but where the transformation is induced by heating. Martensite is stable at lower temperatures, whereas austenite becomes the stable state at higher temperatures. The shape memory effect is created by first setting the desired shape of Nitinol in the austenite phase by heating into the austenite phase. Once cooled back to the martensite phase, the material can be deformed into a new shape. Because of the manner in which martensite deforms (through a mechanism known as 'twinning'), when the material is heated back to the austenite phase it returns to the shape that was originally set in the austenite state, thus having 'shape memory'. Like superelasticity, the shape memory property can be used for deploying components so that they reach a desired shape upon release and as an actuator that can be manipulated through temperature changes. However, to date the superelastic effect of Nitinol is by far the more widely used in the medical device industry [8,9].

The specific properties of Nitinol required for exhibiting superelasticity vs shape memory at a given temperature are different, and thus Nitinol needs to be manufactured

and treated appropriately for a given application. Generally, the temperature at which properties of Nitinol are designed for is body temperature, around 37 °C. For the superelastic transformation from austentite to martensite to be driven mechanically, the Nitinol component needs to be in the austenite state at body temperature and within range of being stable in the martensite state under a reasonably low load. The key property that determines whether this is possible is the transformation temperature between martensite and austenite, known as the austenite finish temperature (A_f), which is the temperature at which austenite is fully formed. The austenite finish temperature should be below body temperature in order for the component to be fully austenitic at body temperature. Figure 2, derived from a review paper by A.R. Pelton, et. al. [10], shows how the difference between the austenite finish temperature, 11 °C for the alloy tested, and the ambient temperature (denoted in a box in each graph) around the Nitinol component affects the mechanical performance. Samples below 0 °C are clearly in the martensite state and do not exhibit superelasticity. Above 0 °C, the material shows evidence of superelasticity (austenite starts to form in this material at -22 °C) with an upper plateau showing a transformation from austenite to martensite and a reverse transformation along the lower plateau upon unloading, returning the material back to near zero strain. The stress at which the upper and lower plateaus occur is often a design criterion for applications, which further constricts what the austenite finish temperature of the Nitinol alloy needs to be. Generally, Nitinol alloys engineered for medical device applications have austenite finish temperatures around 10-40 °C below body temperature to be in the superelastic state.

The transformation properties of Nitinol can be characterized by cycling temperature and measuring the heat released/consumed during the transformation between martensite and austenite, using a method known as differential scanning calorimetry (DSC). Figure 3, also derived from a review article by A.R. Pelton and coworkers [10] shows the output of a typical DSC experiment where key transformation properties such as the austenite finish temperature can be measured for a Nitinol component. The peak from heating (downward facing peak) is the transformation from martensite to austenite, with the material fully in the austenite phase after the peak (describes the austenite finish temperature). Other transformation temperatures play a

role on the mechanical properties of Nitinol as well, but are outside of the scope of this work.

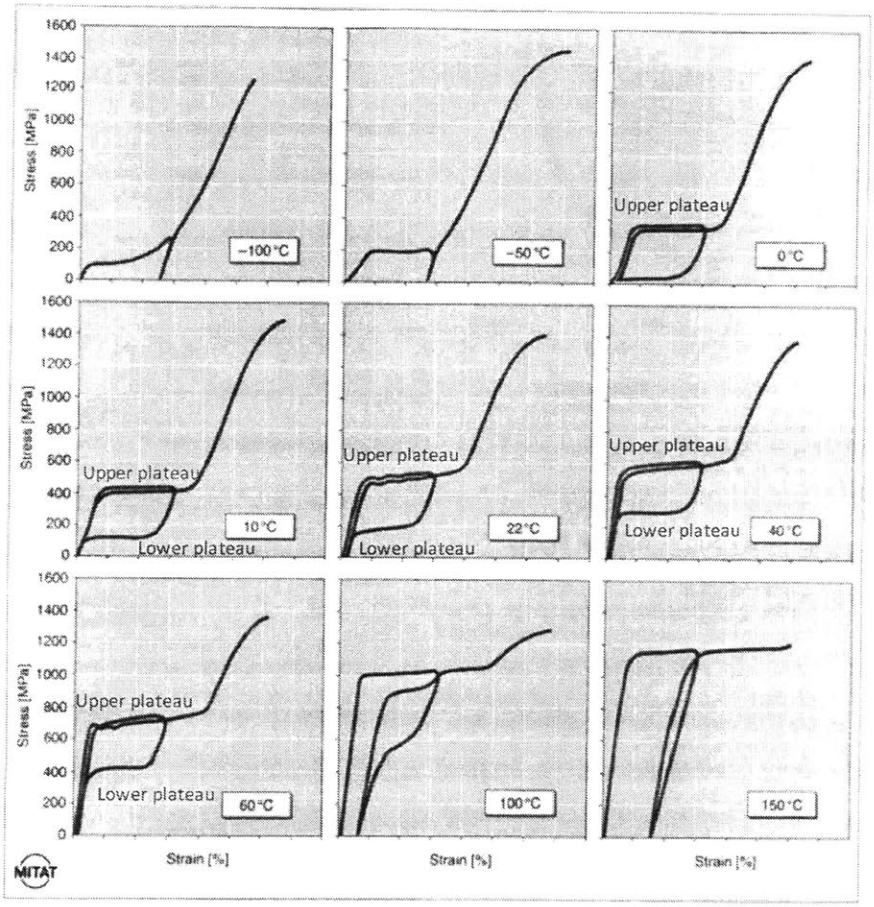

Figure 2. Stress-strain curves showing the mechanical performance of Nitinol with an austenite finish temperature 11 °C tested at different operating/ambient temepratures (reproduced with permission from A.R. Pelton et. al. [10]).

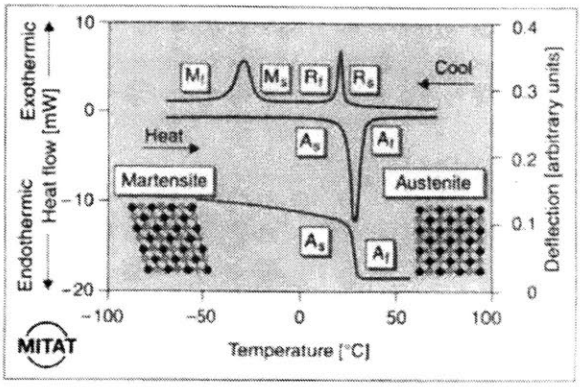

Figure 3. A typical DSC curve (reproduced with permission from A.R. Pelton et. al. [10]).

1.1.2 Current Manufacturing Methods for Nitinol

The superelastic properties of Nitinol are critical to its use over other, more traditional alloys such as steels. As mentioned in the previous section, the ability to elastically deploy parts through hollow wires allows for much less invasive surgeries for both short-term and long-term implantable devices [8,9]. Several other benefits of superelasticity are subtler, such as kink resistance and biomechanical compatibility, which lead to Nitinol being chosen for stents and guidewires for catheters as more reliable alternatives to other alloys [9]. Shape memory properties are also utilized in certain applications where the application of heat can change the shape of the material without requiring invasive surgeries. Examples of shape memory Nitinol include wires in orthodontics and bone plates for fractures [8,9]. A few applications use Nitinol directly in the martensitic state for its ductility, such as the Paragon stent [8].

Manufactured wrought NiTi components for medical devices must meet the American Society for Testing and Materials (ASTM) standards, ASTM F2063, for this material [11]. The standard specifies that the nominal Ni composition must be between 54.5 and 57 wt.%. The Ni composition has a strong effect on the austenite finish temperature [12], with increasing Ni composition leading to a lower austenite finish temperature. Ni compositions in the range specified are expected to yield superelasticity at body temperatures. In addition, the standards specify maximum compositions for

several impurity elements that can be introduced during the manufacturing and materials processing stages. Table 1 shows the limits for these different impurities [11].

Table 1. Impurity element maximum allowances in Nitinol medical devices [11].

Element	Maximum weight percentage
Carbon	0.05
Cobalt	0.05
Copper	0.01
Chromium	0.01
Hydrogen	0.005
Iron	0.05
Niobium	0.025
Nitrogen + Oxygen	0.05

The presence of impurities can embrittle Nitinol alloys, leading to premature failure of the component. Of particular importance, given the traditional manufacturing and processing routes as well as expected exposure in the additive manufacturing process, are the carbon, hydrogen, nitrogen, and oxygen contents. Minimizing the introduction of these elements is an important part of designing the processes for producing Nitinol components.

The conventional manufacturing processes for Nitinol are shown in Figure 4, which is derived from a review article by Elahinia et. al [13]. Ni and Ti are typically alloyed either through a melting and casting process or through powder metallurgy (special processes include processes such as thin films produced by sputtering). Melting requires a vacuum furnace as Ti is a highly reactive element, with vacuum induction melting and vacuum consumable arc melting being the most widely used processes [14]. Both processes have been tuned by controlling the choice of crucible to minimize impurities, the temperature of melting, and the rate of temperature change in casting (usually very slow rates) to produce homogeneous parts with tight control over chemistry in order to reach the desired austenite finish temperature for a particular component.

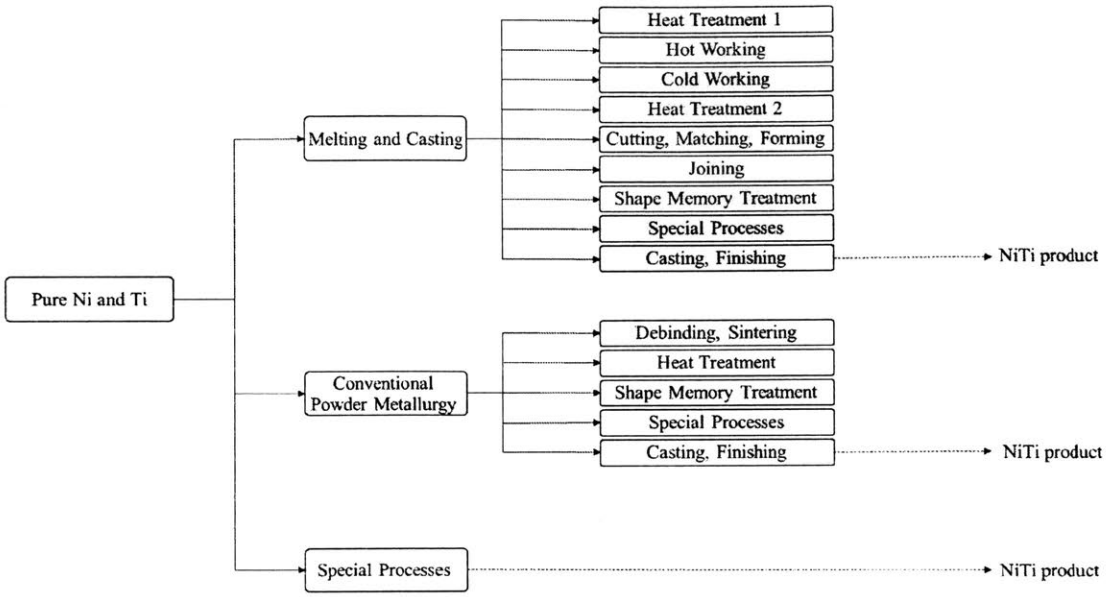

Figure 4. Conventional processing of Nitinol (reproduced with permission from Elahinia et. al. [13]).

The subsequent steps in the process after melting and casting shown in Figure 4 generally aim to affect the microstructure, surface properties and final shape of the Nitinol component. Nitinol is generally first produced into thin wires or tubes from which the resultant part is produced. These steps are generally labor intensive and require delicate engineering to maintain the mechanical properties and superelasticity. Nitinol is a particularly difficult alloy to machine which limits the types of methods that can be used to create the desired shape.

Conventional powder route processing for Nitinol includes sintering (including spark plasma sintering and hot isostatic pressing) and metal injection molding and aims to make components near the desired net shape to reduce the number of manufacturing steps required to produce the final component [15]. Powder is produced generally using gas atomization in order to attain nearly spherical powder particles. Powder generally contains a higher impurity concentration than cast Nitinol ingots due to the higher surface area of the powder, which makes it difficult to control against the formation of oxide and carbide phases that embrittle the alloy [16]. Sintering and metal injection molding can have high porosity due to the difficulty in fully consolidating the powder [17, 18], which has in some cases been used to make porous components for implants. However, in most

Nitinol applications, the presence of pores is another source of embrittlement and can lead to premature failure of the component.

The challenges associated with conventional Nitinol production are instructive to the efforts to produce Nitinol through additive manufacturing. The additive manufacturing technique that is primarily studied for Nitinol is selective laser sintering, which melts together Nitinol powder particles using a laser beam in an argon atmosphere. Ultimately the tantalizing potential of additive manufacturing for Nitinol is to produce parts near net shape to eliminate the costly manufacturing steps for current Nitinol parts and open up the potential for new geometries of Nitinol components. However, the challenges of using powder, which can have higher impurity concentrations and lead to porosity, and relying on a melting and solidification process through the laser which can affect the chemical composition and homogeneity of the part are major components of determining whether additive manufacturing of Nitinol is a viable technology.

1.2. Review of Additive Manufacturing Studies of Nitinol

Additive manufacturing of Nitinol has been studied by materials science researchers over the past 10 years to develop an understanding how the printing process affects the material properties and solve early challenges in creating high quality Nitinol through 3D printing. The most common additive manufacturing technique that is utilized for Nitinol is called selective laser sintering. Selective laser sintering uses a feed of metal powder, in this case Nitinol powder, which is sintered (effectively melted together) by a laser beam. A schematic of the process of selective laser sintering is shown in Figure 5 [15].

The process of selective laser sintering starts with a clean substrate on the "fabrication piston" side of Figure 5. A layer of powder is spread across the substrate by inching up the powder delivery piston and spreading the powder over the powder bed/substrate using a roller or other spreading device. The laser then selectively strikes the powder bed based on the uploaded CAD drawings of the desired part geometry. Key parameters of this process include the laser power (usually limited to a range based on the particular laser equipped on the machine) as well as the speed of the laser and the thickness of the powder layer that is spread across the bed. After the laser is finished with

one layer, the fabrication piston moves down by the specified powder layer thickness parameter and the next layer of powder is brought across by the roller. This process is repeated until the final part is finished.

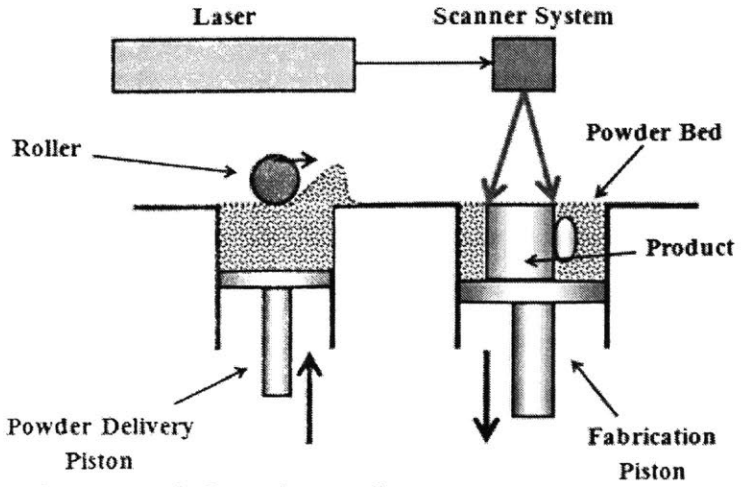

Figure 5. A schematic of the selective laser sintering process, reproduced with permission from Elahinia et. al. [15].

Components built from selective laser sintering have rough surfaces, which generally require surface finishing in post-processing (e.g. wet-blasting or tumbling). In addition, the components are adhered to a substrate and must be removed. Removal from the substrate depends on the part and can be done manually or require the use of an electrical discharge machining wire (EDM wire), which leaves a smooth finish.

While several companies supply selective laser sintering machines [4] with built-in parameter sets for common materials such as copper, titanium, steel, aluminum alloys, etc., developing suitable process parameters for a new material still requires substantial tuning. In addition to the aforementioned laser power and speed parameters, much of the art of 3D printing with selective laser sintering is determining the pattern in which the laser rasters across a layer of the part and interprets the CAD file into a physical laser scanning strategy. The laser scanning strategy (a sample of different common ones are shown in Figure 6 which is derived from the work of Cheng et. al. [19]), for example, determines in what order the different areas of a part in a given layer are melted. The order in which parts are melted effects the thermal history that the material experiences

and can effect microstructural features (such as grain size), internal stresses (which cause warping) from heating and cooling unevenly, and the pickup of impurities. Within each strategy, the distance between consecutive laser passes in the same area is known as the hatch spacing (i.e. the distance between lines in Figure 6), which also has a strong effect on the thermal history and ultimate performance of the printed components.

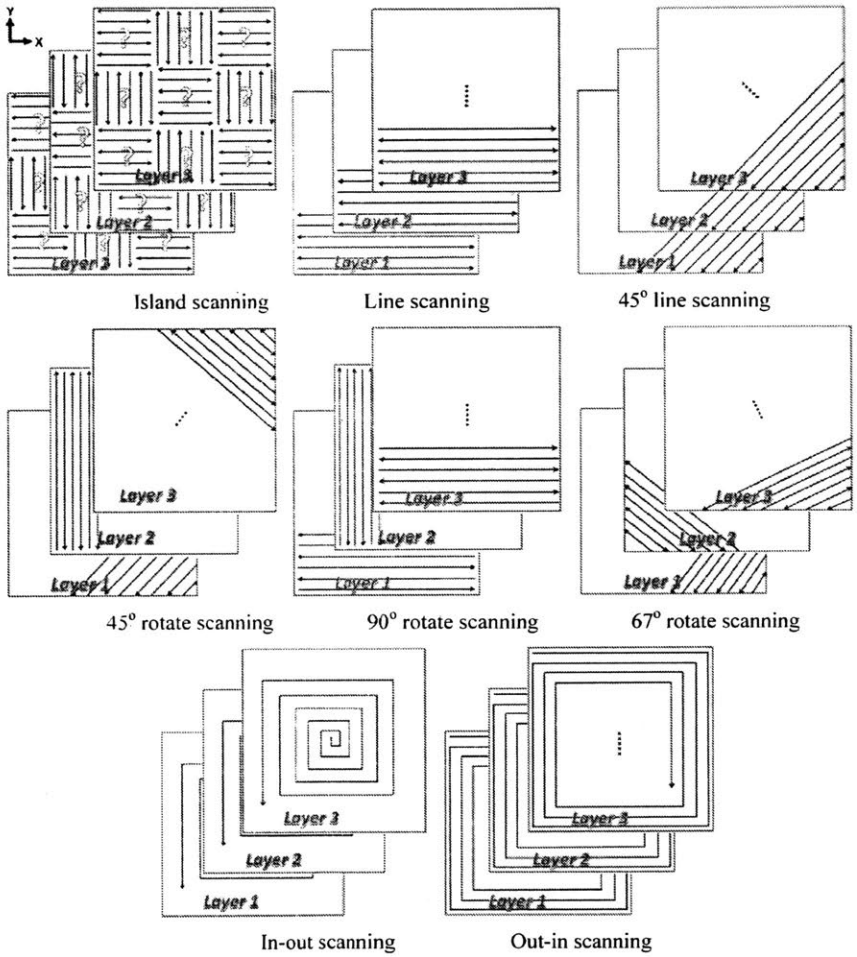

Figure 6. Laser scanning strategies for the body of selective laser sintering components, which can effect internal stresses, surface finish and the presence of porosity in the part (reproduced with permission from Cheng. et. al [19]).

In addition, scanning strategies for the surface layer of the part often differ, referred to as contour scans, which often have unique laser parameters to attain better surface finish and dimensional tolerance. Similarly, the first few layers binding the part to the substrate can

have different strategies to make the removal of the component after printing easier or to ensure rigidity during the printing process.

Selective laser sintering is well suited for a wide range of material components, from plastics to metals and ceramics, which has led to it being the prime method for exploring Nitinol 3D printing [20-44]. Other methods such as directed energy deposition that are flow based have also been explored [45-48], but are not considered in this work. The remainder of this section highlights the findings of several research groups that have studied 3D printing of Nitinol using selective laser sintering [20-44].

The first key attributes of Nitinol that are generally necessary (i.e. regardless of particular application) is to be able to print components with sufficient density and chemical control, as these material properties are required for ductile, superelastic, and shape memory parts. Figure 7 is a summary of laser power and scan speed parameters for selective laser sintering that have been studied [20-44].

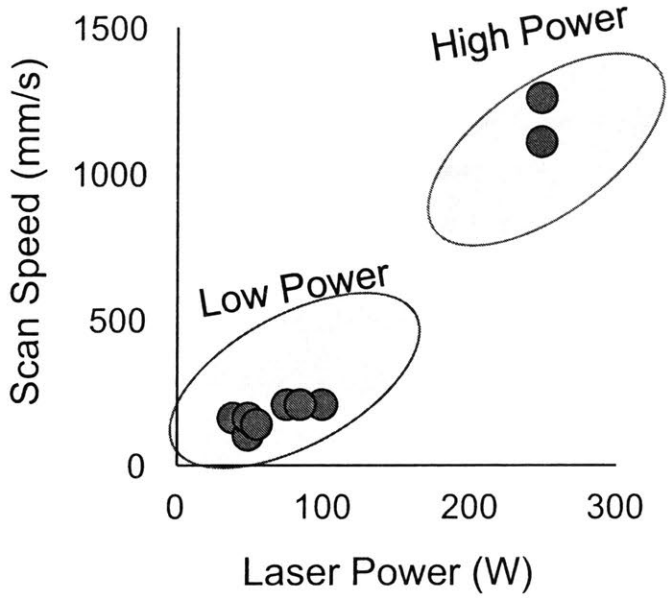

Figure 7. A summary of laser power and scan speeds used for selective laser sintering of Nitinol, with two distinct regimes emerging: a low power regime with powers between 40-100 W and a high power regime with powers over 200 W [20-44].

The printing parameters fall into two regimes. Most studies have been conducted in the 40-100 W regime of power with correspondingly low scan speeds. This power range reflects the operating power range of most commercial selective laser sintering machines. A select few studies have been conducted at very high powers of 250 W using specialized selective laser sintering equipment. Dadbakhsh and coworkers [42] summarized the different output properties from printing parameters in these different ranges. In both regimes high relative density components of greater than 99% were found (a high relative density means that the material has few pores or voids). In addition, they found that lower scan speeds generally lead to higher transformation temperatures, which naturally lends these parts to be more useful for shape memory applications than superelastic applications.

This effect of the printing parameters on the transformation temperatures, most critically the austenite finish temperature, is critical to the viability of Nitinol additive manufacturing. In earlier work, Dadbakhsh and coworkers studied this effect using high power laser parameters and low power laser parameters, resulting in the DSC curves shown in Figure 8 [40].

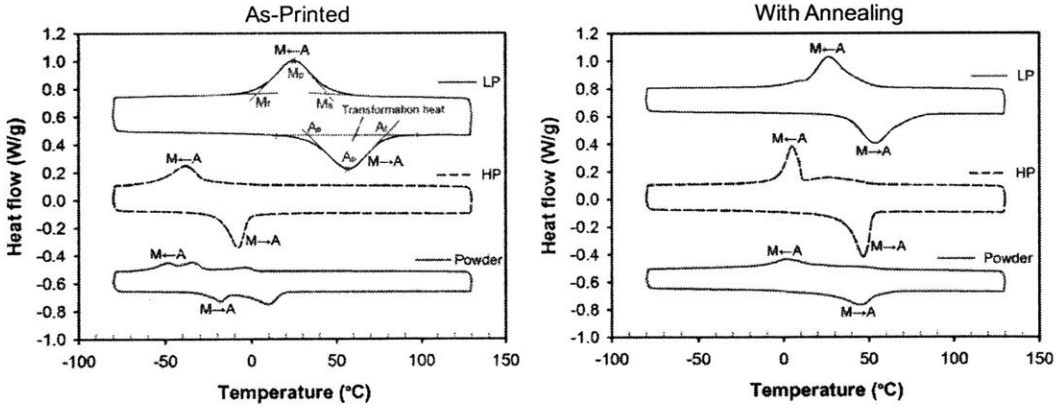

Figure 8. DSC curves for selective laser sintered parts under low (40 W) and high power (250 W) laser settings (reproduced with permission from Dadbakhsh et. al. [40]).

The DSC curves for the as-printed and virgin powder (on the left in Figure 8) show a marked shift of the transformation peaks to higher temperatures at low power printing parameters. The austenite finish temperature reaches around 80 °C from a virgin

powder with an austenite finish temperature closer to 20 °C, which would be appropriate for superelastic Nitinol products at body temperature. Upon annealing the powder and the printed parts at 830 °C for 25 minutes, the authors note that the low power curve is no longer shifted relative to the powder's DSC curve. Trends similar to this are observed in several studies of Nitinol selective laser sintering.

Based on these results, Dadbakhsh and coworkers identify several possible reasons for the increase in the transformation temperatures when printing the component at low power:

1) Preferential evaporation of Ni during printing due to the higher vapor pressure of Ni which would lower the Ni content of the printed part and lead to a higher austenite finish temperature.
2) Precipitation of secondary phases of Ni, such as Ni_4Ti_3, which would decrease the Ni content in the rest of the part and also lead to internal stresses and barriers to the phase transformation.
3) Smaller grains due to the different cooling rate which can affect the transformation temperatures, and
4) Residual stresses and grain textures which can affect the transformation temperatures.

In their work, Dadbakhsh and coworkers claim that precipitation is the most likely cause for the increase in the transformation temperature as evidenced by the lack of differences in the transformation temperatures in the annealed structures. However, the root cause differs between different authors who have studied the increase in transformation temperatures. Bormann et. al. and Haberland and coworkers instead attribute the change in transformation temperatures to a loss in Ni content [23, 49], but do not present corroborating data measuring the loss of Ni to correlate with the observed increase in the transformation temperatures.

One of the main goals of this work is to understand whether Nitinol can be printed on commercial selective laser sintering machines, which means printing at less than 200 W, with superelasticity at body temperature. As part of this goal, the experiments should shed further light into the root cause for the increase in transformation temperatures that have been observed by others (Section 3.4.4).

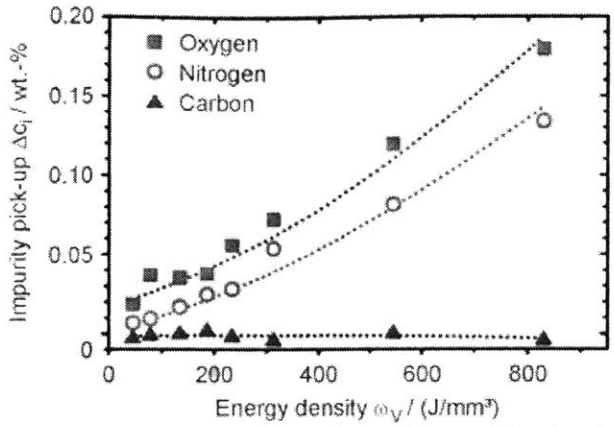

Figure 9. Effect of printing parameters on the pickup of impurities in the printed parts (reproduced with permission from Haberland et. al. [23]).

Another important factor that has been studied is the introduction of impurities during the printing process. During the laser sintering process, the material reaches its melting temperature and is susceptible to dissolve impurity species from the surrounding atmosphere or from the substrate. The atmosphere used is an argon atmosphere, but still contains oxygen and nitrogen in enough content to be introduced into the melt pool. Figure 9 from a study by Haberland et. al. [23] shows how the pickup of air elements in the argon atmosphere – oxygen and nitrogen – increase with the amount of energy introduced by the laser into the melt pool (energy is calculated based on the power of the laser and how long it sits over a particular area of the material). Using different methods to cycle the argon gas in printing chamber, Haberland et. al. [23] show that the increase in oxygen and nitrogen content can be minimized to be in line with conventional Nitinol ingots. In this thesis, the impurity contents of printed Nitinol will also be a subject of study in determining whether parts can be consistently made to meet the ASTM F2063 standards for impurity content using commercial Nitinol powder as feedstock.

2. Thesis Outline

The ability to 3D print Nitinol components offers a new manufacturing route that can reduce costs for printing medical devices with complex geometries and opens up the opportunity for entirely new medical devices that could not previously be fabricated. As outlined in the Section 1.2, early research has been conducted by materials scientists to determine whether Nitinol can be fabricated using selective laser sintering in a lab setting. The research highlighted optimism in the ability to produce dense components and identified concerns regarding impurity content and an increase in the transformation temperatures of Nitinol.

This thesis begins by building on the academic studies exploring this technology to assess the feasibility of printing Nitinol components of medical grade in an industrial setting. The engineering assessment (Section 3) identifies the main performance metrics required in Nitinol medical device components, produces experimental results to determine whether these performance metrics can be met using selective laser sintering, and reveals the main challenges that remain for adoption of this technology in the medical device industry.

The engineering assessment is then used to explore the business case for 3D printed Nitinol for medical devices. The relative difficulty of achieving different engineering properties is used to identify the most likely applications for using this technology in the near future. A cost accounting model is developed for Nitinol to understand the operational and financial aspects of investing in Nitinol 3D printing and to identify the different costs associated with different routes of implementing this technology. This model is used to identify the general sizes and types of components that are most likely to experience large cost advantages over traditional Nitinol manufacturing.

This work was done with Boston Scientific, a leading medical device producer, headquartered in Maple Grove, MN. The work was primarily completed in Clonmel, Ireland.

3. Assessing Feasibility of Producing Quality Nitinol Components

3.1 Developing design targets for 3D printed Nitinol

Table 2 shows a summary of the main engineering properties that are considered in evaluating the quality of 3D printed Nitinol components. The stakeholders for this project include product development engineers, research and development scientists, and regulatory agencies (using the standards described in ASTM F2063 for Nitinol medical device components [11]). The majority of the properties that need to be met are mechanical properties, as it is the mechanical properties of Nitinol that make it a useful candidate for medical devices. In particular, the yield strength, % elongation at failure, % plastic strain after recovery, and # of cycles to failure were identified as critical properties for which to meet specifications for a broad range of medical device applications.

Table 2. Engineering properties of Nitinol that should be considered in evaluating the performance of printed components

Property	Type of Property	Importance to Stakeholders
Yield strength	*Mechanical*	*High*
% elongation to fracture	*Mechanical*	*High*
% plastic strain after recovery	*Mechanical*	*High*
Upper plateau strength	*Mechanical*	*Moderate*
Lower plateau strength	*Mechanical*	*Moderate*
Ultimate tensile strength	*Mechanical*	*Low*
Young's modulus	*Mechanical*	*Low*
Shape memory effect extent	*Mechanical*	*Low*
# of cycles to failure	*Mechanical – Fatigue*	*High*
Dimensional tolerances	*Geometrical*	*High*
Corrosion resistance	*Chemical*	*High*
Biocompatibility	*Chemical*	*High*

The yield strength describes the maximum stress that the component can experience before it is permanently deformed (also known as plastic deformation). Plastic deformation is an important failure criterion for medical device components as once the

part is permanently deformed it will no longer perform its function in the manner in which it was designed. The % elongation to fracture describes the maximum strain that the material can experience before breaking. In the context of Nitinol this property is important mostly as it reflects the type of failure mode that occurs in these components. A % elongation that is too low can mean that the part is susceptible to undergo brittle fracture, as opposed to ductile fracture which allows for plastic deformation before failure and is generally required for medical device applications. The % elongation under elastic strain is also very important in Nitinol as it relates to its superelastic property. This property is captured in Table 2 as % plastic strain after recovery, which is the amount of permanent deformation that occurs in the component after the part has been deformed to a fixed strain and released. The fixed strain for deformation can vary based on the application, but is often set at 6% elongation for consistency across tests. For applications where fatigue plays an important role – which can broadly be described as any component that is used as a long-term implant – the # of strain cycles that the component can endure before failure is critical as it determines how long the component can remain in the body before fracture. The fatigue life of traditionally manufactured Nitinol is often cited as one of the most challenging engineering properties to achieve and is thus also likely to be one of the main challenges for 3D printed Nitinol [43], as 3D printing as a manufacturing technique is generally poor at achieving good fatigue properties.

In addition to mechanical properties, the dimensional tolerances of the components are critical to meeting the engineering requirements of Nitinol applications, which utilize fine features as is typical in the medical device industry (many critical feature sizes will be 10s to 100s of microns and each critical feature must be inspected to meet regulatory standards). Biocompatability is also an important consideration as Ni is toxic, and so careful design of the surface treatment of the part is required to ensure no Ni diffusion into the body.

The experiments in Section 3.4 are designed to identify the relative difficulty of achieving the different properties in Table 2.

3.2 Identifying key tunable process parameters in the additive process

The properties of the printed Nitinol components will depend strongly on the process parameters used to 3D print Nitinol parts. Table 3 shows the most significant process parameters in the selective laser sintering process.

Table 3. Process parameters in the selective laser sintering process that need to be tuned to achieve high performance Nitinol parts.

Process Parameter	Process Phase
Nitinol powder size & shape	*Raw Material*
Nitinol powder chemistry	*Raw Material*
Laser power	*Printing*
Laser scan speed	*Printing*
Laser scan pattern	*Printing*
Layer thickness	*Printing*
Support structure geometries	*Printing*
Printing atmosphere	*Printing*
Solution annealing	*Post Processing*
Electropolishing	*Post Processing*
EDM wiring	*Post Processing*

The Nitinol powder is a critical input into the selective laser sintering process. The properties of the Nitinol powder depend strongly on the properties of the original wire that is used in gas atomization, particularly the chemistry, which includes the concentrations of Ni and Ti as well as the presence of impurities such as oxygen, nitrogen, carbon, and hydrogen which can have a very strong affect on the properties of the 3D printed component. While the powder properties are very important, as a medical device producer, testing various powders in a rapid manner is challenging as Nitinol powder is a relatively scarce resource with very few suppliers. Nitinol powder lead times are generally between 3 to 6 months.

Within the selective laser sintering process, several machine parameters can be tuned to perform a design of experiment to optimize around the desired properties. The

most common parameters that are used are the laser power, laser speed, and the laser scan strategy, which is often simplified to specify the distance between laser scans (called the hatch spacing). The amount of powder that flows onto the bed between recoats is determined by the layer thickness. In addition, the actual quality of the printing atmosphere can be particularly important for Nitinol where lower oxygen content is required (the ASTM F2063 specification for oxygen content is 0.05 wt%).

After printing, various post-processing techniques can be used to bring properties in line with the desired specifications. Solution annealing has been shown in several studies of 3D printed Nitinol [23,31,33,40] to help provide better superelastic properties. Solution annealing is performed by raising the temperature of the part up to an elevated temperature where various Ni,Ti compounds will dissolve and grains often will recrystallize to yield a more preferred grain structure. Subsequent annealing has also been shown to be useful to produce some desired precipitates [23,31].

The surface finish for traditionally manufactured Nitinol components is often provided by electropolishing and is thus an important potential step in producing high quality 3D printed Nitinol as well. For all parts, the printed component needs to be removed from the substrate, which is often done using an EDM wire, which can create localized heating on the cut surface.

Several of these parameters are studied in Section 3.4 to determine the most critical processing parameters for producing quality Nitinol components and to characterize the highest quality components produced.

3.3. Identifying fundamental material properties that link processing parameters to desired properties for Nitinol produced by selective laser sintering

While Table 2 provides the properties of Nitinol that directly relate to the performance of the printed alloy, there are important material properties of Nitinol components that, while indirectly affecting the mechanical and functional properties of the alloy, are more direct consequences of the manufacturing process. In metallurgy, these relationships are called Process-Structure-Property relationships [50], where the process parameters in a manufacturing process directly affect the material at a structural level, and it is these material properties that directly cause the mechanical and functional

properties of the part. Figure 10 shows the Process-Structure-Property relationships for selective laser sintering of Nitinol.

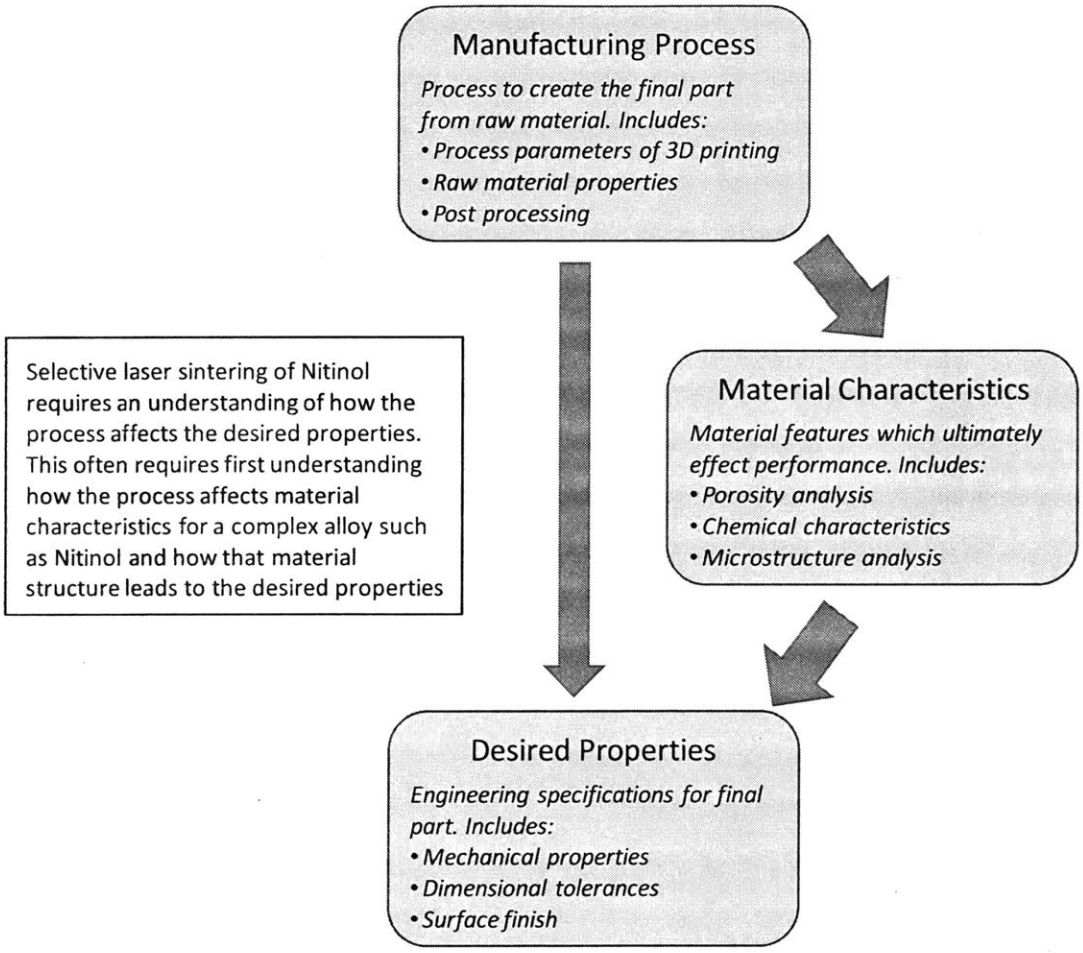

Figure 10. Schematic of engineering feasibility analysis of producing Nitinol using selective laser sintering

The important role that these structural features, or material characteristics in Figure 10, play in understanding the feasibility of producing engineering quality Nitinol through selective laser sintering can be understood by looking at the characteristics listed Table 4.

Table 4. Material characteristics of Nitinol that can help understand how the 3D printing process affects the engineering properties of 3D printed Nitinol

Material Property	Strongly related engineering properties
Relative density	*% elongation to failure, # cycles to failure*
Max pore size	*% elongation to failure, # cycles to failure*
Surface quality	*% elongation to failure, dimensional tolerance*
Impurity concentration	*% elongation to failure, # cycles to failure*
Max inclusion size	*% elongation to failure, upper/lower plateau*
Grain size	*Yield strength, upper/lower plateau, % recovery*
Precipitated phase chemistry	*upper/lower plateau, yield strength, % recovery*
Ni to Ti ratio	*Upper/lower plateau, % recovery*
Transformation temperature	*Upper/lower plateau, % recovery, (also depends on other material properties strongly)*

The first two properties are relative density and maximum pore size, which both speak to the presence of defects in printed components. The presence of defects in the printed component is known to depend strongly on several processing parameters in Table 3. For example, if the laser power during the printing process is too low, the powder will not melt sufficiently leading to cavities in the part where the melted powder does not flow to fill. The presence of pores then directly affects mechanical properties. Substantial porosity in a component can lead to brittle fracture of the part, since the pore can be a natural place for cracks to initiate and propagate, which leads to a low % elongation to fracture. To prevent brittle fracture, the part should have a high relative density (which speaks to the average porosity) and small pores overall.

The surface finish in particular is an important challenge in 3D printing as the components as-printed will have a surface roughness that will generally be outside of the specifications of the dimensional tolerances of parts. The tight dimensional tolerances can be difficult to meet when surface roughness causes significant variance in the dimension throughout the part. For Nitinol in particular the surface finish also must meet chemical requirements in order to assure biocompatibility of the parts and a high corrosion resistance. Ni is a toxic element and it is the oxide that forms on the surface of Nitinol that allows it to be used safely as an implant. A rough surface is also a fertile ground for crack initiation which can lead to brittle fracture.

The impurity concentration in Nitinol is another important material characteristic for all Nitinol medical device components. Standards for Nitinol specify maximum concentrations of oxygen, carbon, hydrogen, and nitrogen among other impurities [11]. Each of these elements can play two roles that, like porosity, can lead to premature failure of the components through brittle fracture. Each of these impurity elements can form various compounds, or inclusions, for example titanium carbide (TiC) and titanium dioxide (TiO_2), which are very hard phases formed within the part and form interfaces that are highly susceptible to brittle fracture. These elements can also segregate to grain boundaries – interfaces between neighboring grains in the alloy – and weaken the bonding along that interface. This process is known as grain boundary embrittlement and these elements, particularly hydrogen, are potential embrittlers in Nitinol [51]. During the printing process, when powder is melted it reaches high temperatures where impurities have a much higher solubility in the metal. When the part is cooled, the components can retain higher concentrations of these elements which leads to the aforementioned issues.

A few processing parameters play a critical role in the impurity content of the resulting components and the maximum size of any inclusions that form as a result. First, the raw powder itself should be as impurity free as possible, as impurity concentrations will only increase during the printing process. Secondly, the printing atmosphere, which in the commercial selective laser sintering machines considered here is typically an argon atmosphere, should have low impurity concentration and be circulated in the machine in a manner that minimizes exposure of impurity elements to the part [23]. Finally, the laser speed, power and scan strategy affect how long the part stays in the melted state and how fast it cools. A higher laser power and faster scan speed generally yield a lower concentration of impurities as the high laser power heats the material quickly and the fast laser speed moves the heat away from the part quickly allowing it to cool faster.

The grain size and the presence of any precipitated phases affect the yield strength of the part as well as the phase transformation that leads to superelasticity. The presence of smaller grains and many small precipitates can make the material harder – as the interfaces add strength to the material [52] – but can also make it harder for the material to transform. Precipitated phases in NiTi occur when regions of the material are off-stoichiometry and thus other stable phases can be formed as described in the Nitinol

phase diagram. These properties will be affected by the original chemistry of the powder as well as the printing parameters which affect the rate at which the material is heated and cooled.

The superelastic properties of Nitinol depend strongly on the concentrations of Ni and Ti in the NiTi phase [12], where increasing the amount of Ni can increase the temperature at which the phase transformation occurs significantly. The temperature at which martensite transforms to austenite is a critical material characteristic/functional property as superelasticity only occurs when the part is in the austenite phase (i.e. above the austenite temperature). For medical device applications, the material needs to be in the austenite phase at body temperature of 37 °C in order for superelasticity to occur. The difference between the phase transformation temperature and the temperature under which superelasticity is being tested determines where the upper and lower plateau stresses lie, which makes understanding where the transformation temperature occurs very important.

The transformation temperature is affected by the processing parameters in many ways. As mentioned, the relative concentrations of Ni and Ti affect the transformation temperatures. The presence of precipitated phases can preferentially consume Ni or Ti which changes their concentration in the NiTi phase. Ni has also been hypothesized to evaporate preferentially [23, 49] to Ti during the selective laser sintering process, which again will depend on the the rate of heating and cooling. Transformation temperatures can also be dependent on residual stresses present in the 3D printed component which are common in 3D printed parts. These effects are discussed in more detail in Section 1.2.

Characterizing these material/structural properties is a critical step to understanding the challenges associated with selective laser sintering and is the fundamental driver behind the design of the experiments shown in Figure 12. The experiments focus primarily on the printing and post-processing parameters as opposed to the raw powder parameters, due to the aforementioned long lead times of sourcing multiple types of Nitinol powder. The experiments focus on addressing the mechanical properties in the most detail, as these properties are the most fundamental to the use of Nitinol in the medical device industry. To link these process parameters and mechanical

properties, parts will be characterized to study the level of porosity, surface roughness, transformation temperatures, and chemical concentrations.

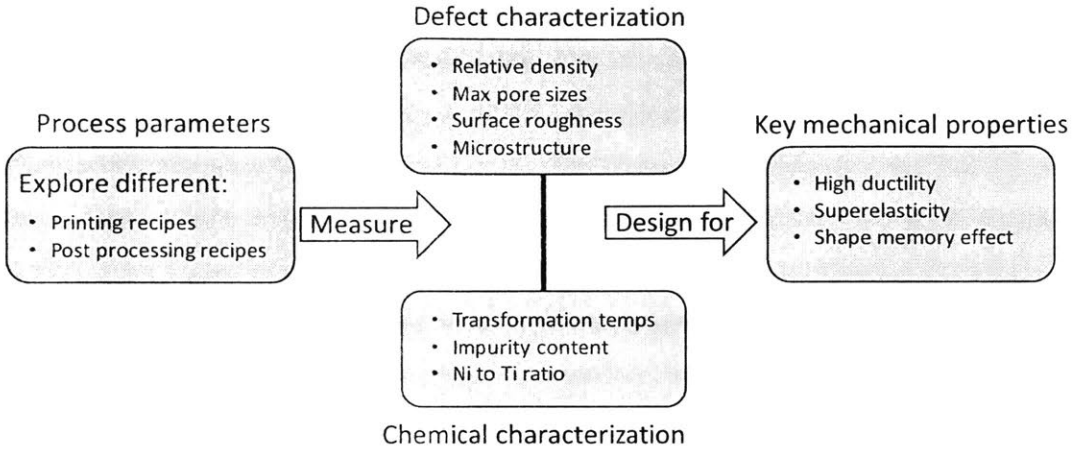

Figure 12. Flow chart of the experimental assessment of the feasibility of 3D printing Nitinol components in Section 3.4.

3.4. Experimental analysis of the feasibility of 3D printing Nitinol using selective laser sintering

3.4.1. Methodology

Printing of Nitinol coupons was done on commercial selective laser sintering machines with the range of allowable laser powers ranging up to 100 W. Printing parameters were varied based on values provided in previous studies in the literature [20-44] (Figure 7). Using these values as initial seeds, further exploration was done using a basic square grid exploration of the printing parameter space. Post process annealing was conducted using a vacuum furnace, and annealing temperatures were determined based on the literature as well [20-44].

The porosity of components was measured mounting printed parts in an epoxy resin and polishing the samples to achieve a mirror finish. Polished samples were then analyzed using an optical microscope with 5x to 100x magnification. Surface roughness was measured by sending components to a scanning electron microscopy (SEM) service provider. Surface roughness of parts were studied before and after electropolishing, where electropolishing was also conducted through a service provider. Electropolishing

was done to varying extents, leading to different levels of mass loss from 5-30%. Chemical analysis using inductively coupled plasma mass spectrometry was conducted by a single service provider for sintered parts as well as the virgin powder.

Differential scanning calorimetry (DSC) was conducted on the virgin powder and the printed components, with and without post processing using an in-house DSC machine. The transformation temperatures were determined using a standard heating and cooling rate of 10 °C per minute using straight lines along the peaks to determine precise temperature of the key transformation points (see Figure 8 for an example). Multiple cycles were conducted to ensure no change in transformation temperature due to thermal cycling in the temperature range considered.

Precise details of the above testing apparatuses and protocols, and similarly the quantitative results from the testing, are withheld to protect the interests of Boston Scientific.

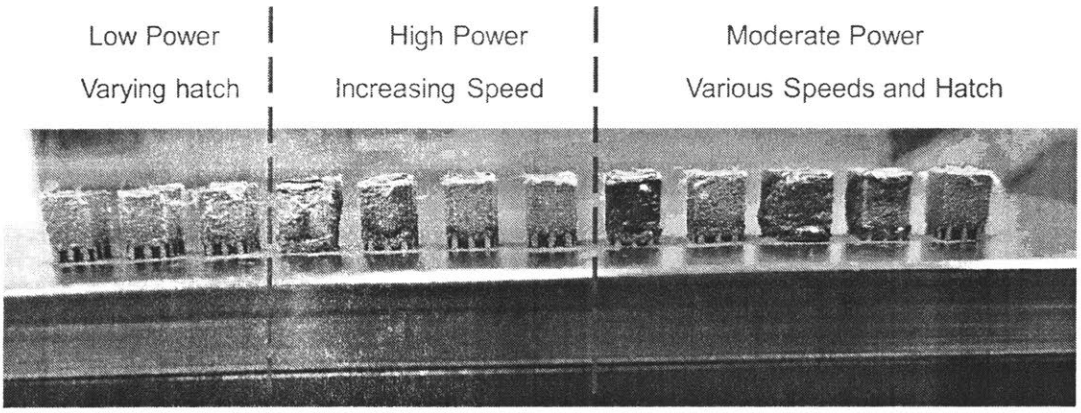

Figure 13. 3D printed test coupons to study effect of printing parameters on material properties

3.4.2. Analysis of density and porosity

From the printing parameter exploration, a few sets of parameters achieved relative densities over the required specification set at the outset of this study. The printed components in Figure 13 illustrate the various different types of printed components that were produced. Components that were a clean, gray color, are ones where the printing parameters were close to optimal when printed, with slightly varying differences in the

relative density observed. Parts with coloration due to the large presence of impurities were printed with parameters that lead to overheating, which required either a lower power or faster speed to reach the desired level of density.

Figure 14 shows optical images of internal regions 3D printed Nitinol parts with high relative densities. Very few pores are observed in the high quality printed components with most pores smaller than 50 microns in size.

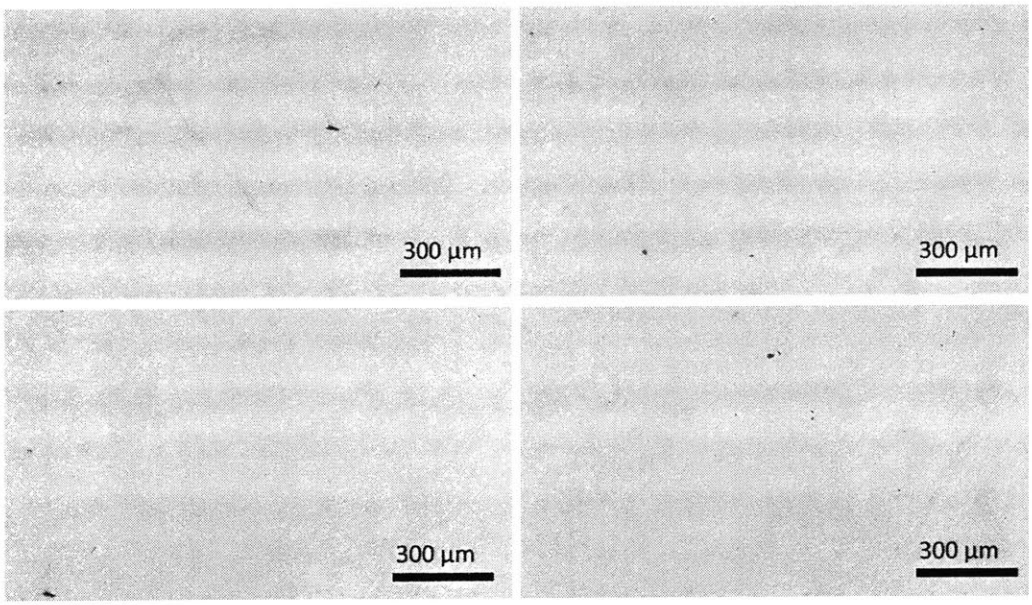

Figure 14. Optical microscope images of polished, printed NiTi samples to study porosity and defects

The ability to achieve parts with this level of relative density is an early indication that 3D printing of Nitinol has the potential to be feasible, along the lines of more conventional 3D printed alloys for medical devices such as titanium and steel alloys. To achieve dense components, several parts of the process must be in-line:

1) The powder should flow uniformly over the plate. If the powder in the bed is not uniform, the parts will have large voids.
2) The weld pool, created by the laser as it melts the powder, needs to be stable and avoid defects such as keyholes.
3) The parts should print without warping due to thermal stresses, which can cause bending in the part as it prints and also lead to defects.

The quality of Nitinol powder that is commercially available and the knowledge developed around viable printing parameters in the literature provides a strong basis to achieve dense components of this material at this stage.

Figure 15 shows optical images of high density parts near the surface. The image on the left shows a relatively rough surface, which is roughly in-line with the roughness of other metals printed using selective laser sintering. In some areas near the edges of the parts, the size of pores increases and the relative density decreases. Thus, while the overall relative density of these components meet the standards, these local pockets can be responsible for a lower fracture toughness in these components. Future work in optimizing the selective laser sintering parameters around density can work on the contour laser parameters – which are often defined differently from the parameters used in the bulk of the part – to reduce the number of pores in these near-surface areas.

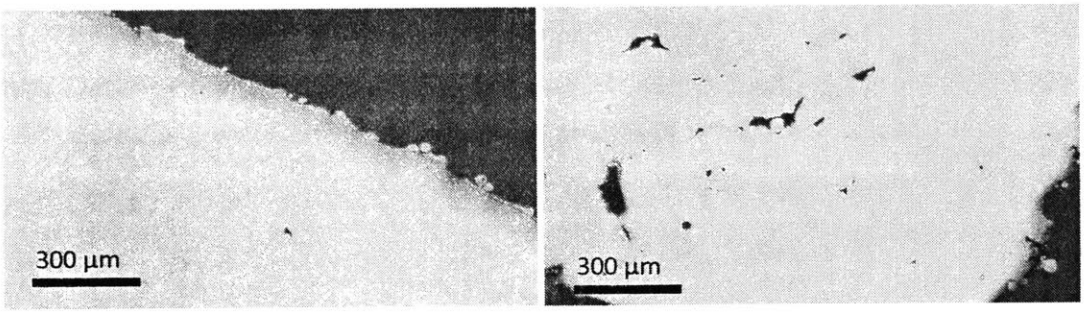

Figure 15. Optical microscope images of subsurface features in polished, printed NiTi samples

3.4.3. Analysis of surface quality and microstrcucture

The surface quality was further studied using SEM to qualitatively determine the extent of surface roughness and provide a comparison to surface quality after surface treatment. Figure 16 shows two surfaces on the as-printed Nitinol component: 1) the surface from the side-view of the part and a surface from the bottom of the part where the part is EDM wired off of the printing platform. Comparing these two surfaces, the printed surface shows substantial roughness over the EDM wired surface. This shows the dramatic difference in surface quality from an as-printed surface to one that has undergone post-processing.

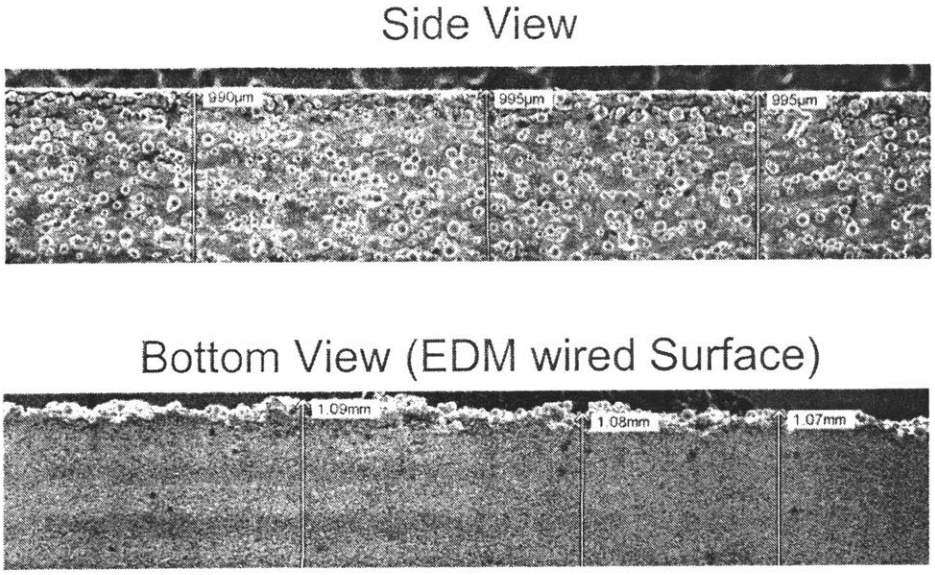

Figure 16. SEM images of two surfaces on the 3D printed Nitinol component with the best density to study surface roughness

The surface quality of a part produced by selective laser sintering can be improved using a number of different post-processing treatments. EDM wiring, while able to provide a good surface quality, is not suitable for the geometries of most printed components. Mechanical treatment of the parts can be achieved using processes such as tumbling or wet blasting where the non uniform areas of the surface are treated by wearing the part using external media.

For Nitinol, electrochemical treatment of the surface using electropolishing is generally used for medical devices as it not only can provide an improved surface quality but it can also help produce the desired outer oxide coating to ensure that Ni does not diffuse out of the part. Figure 17 shows the SEM images of the same two surfaces after electropolishing up to a roughly 10% mass loss in the component.

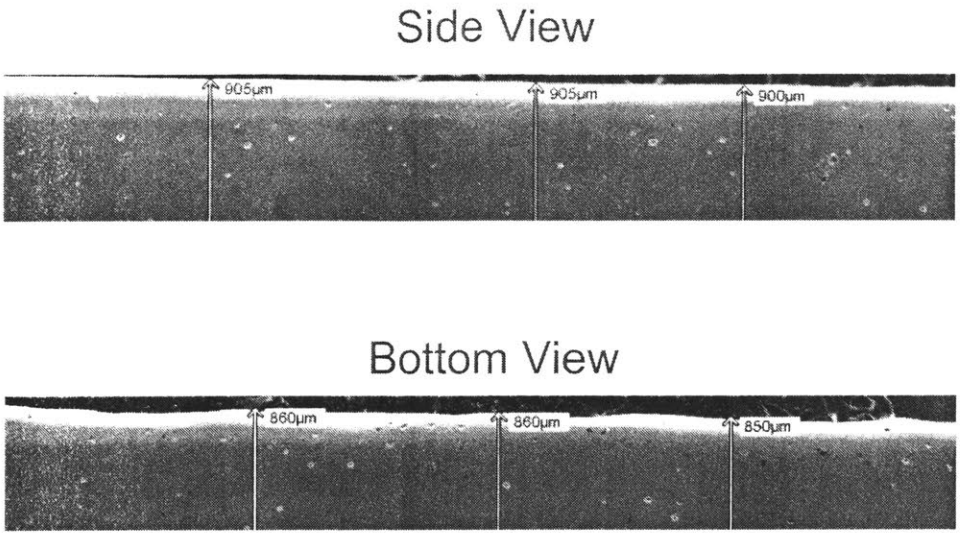

Figure 17. SEM images of two surfaces on the same 3D printed NiTi component as in Figure 16 after electropolishing

There are a number of interesting outcomes from electropolishing to treat the surface of printed Nitinol. First, the surface is much cleaner than the side surface shown in Figure 16, which shows that electropolishing can treat surface roughness reasonably well. However, the surface roughness treated here is more the localized surface roughness than the overall straightness of the surface over the length of the part. In other words, if the surface is considered to be a wave, the frequency of the wave is clearly decreased by electropolishing, but the amplitude of this wave is not clearly affected. The lines drawn to measure the size of the part at different points along the length of the Nitinol coupon show similar variation in both electropolished and as-printed coupons, suggesting that this treatment will likely not help increase how precise of a dimensional tolerance these printed parts can satisfy.

Another effect of electropolishing of printed components is a faceting of sharp edges. Traditionally manufactured Nitinol rarely has sharp edges as the components are predominantly formed from wires and tubes. The parts printed here were rectangular to start and sharp edges were removed during the electropolishing process. Some level of faceting is unavoidable during surface treatments, whether it is a mechanical or electrochemical treatment and needs to be considered a constraint in design of 3D printed

Nitinol components (for example when evaluating designs for parts that will be fitted together).

Electropolishing also reveals pitting within the components, which provides further understanding of the microstructure of 3D printed Nitinol. Pitting due to electropolishing can be revealed here for two primary reasons: 1) the electropolishing of the surface is revealing subsurface pores of the variety seen in Figure 15 and 2) electropolishing of certain elements is preferential, which means that the chemistry of the part is not completely homogeneous. Pitting was observed in parts uniformly throughout the range of electropolishing that was conducted, up to a maximum of 30% mass loss and revealed much more pitting compared to pores that were observed after polishing. There is therefore reason to suspect that some form of precipitation is occurring in these components, which will be discussed in more detail in Section 3.4.6.

3.4.4 Analysis of the phase transformation properties of printed Nitinol

The printing parameters in the first set of testing was designed around optimizing the relative density of the parts and reducing the influence of pores. However, the unique properties of Nitinol rely on the printed components having suitable phase transformation characteristics to demonstrate superelasticity at body temperature, which is a property that is independent of the porosity in the part as it depends most strongly on the chemistry of the part (see Section 1.1.1).

Figure 18 shows the results of differential scanning calorimetry of the virgin Nitinol powder and a printed Nitinol component with high relative density. The x-axis of these graphs shows the temperature, which as shown in the bottom image is varied by heating and cooling the part. The y-axis measures the amount of heat produced or consumed as the temperature is ramped. If there are no transformations, the output will look effectively like a box, with two flat lines, with the bottom line produced during heating and the upper line produced during cooling.

For the raw powder, during heating there are two peaks that form (bottom line in the raw powder graph). The two peaks indicate that an intermediate phase, termed the R-phase, forms between the original martensite phase and the high temperature austenite phase, similar to Figure 3 of DSC curves from Pelton et. al [10]. Upon cooling, there are

still two peaks, though heavily overlapped suggesting that the R-phase forms both upon heating and cooling. The presence of the R-phase generally means that superelasticity is harder to achieve as two phases can form during the phase transformation instead of the single desired martensite phase. While the transformation temperatures for the virgin powder cannot be specified (to protect Boston Scientific's intellectual property), they are roughly in-line with the desired transformation temperatures for a Nitinol alloy.

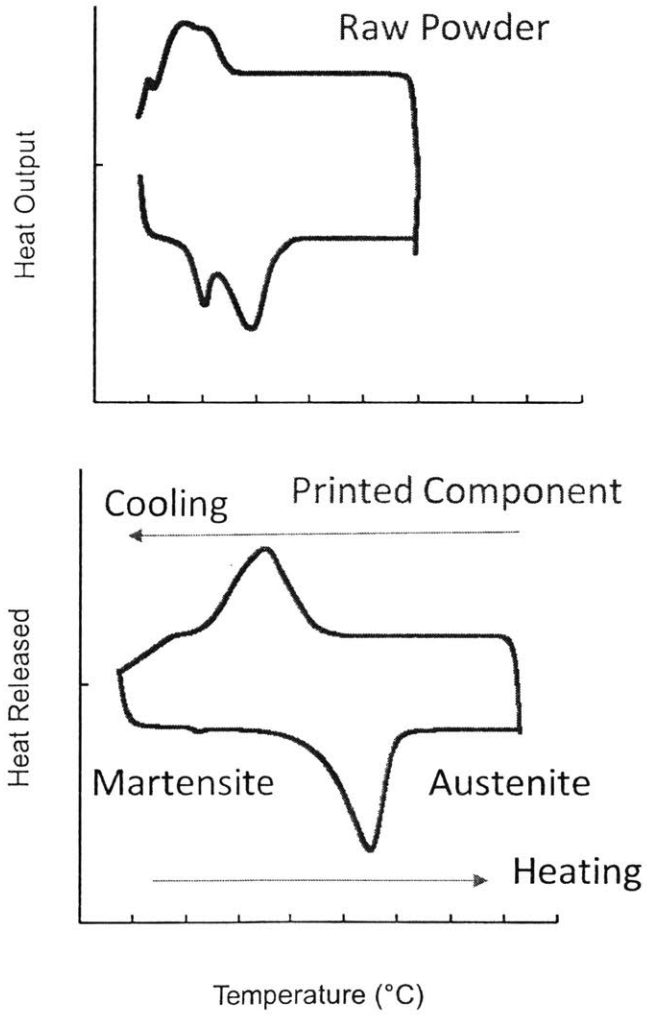

Figure 18. DSC of Nitinol powder (top) and the printed Nitinol component with the best density (bottom). The peaks in the curves shift to higher temperatures through the printing process

The selective laser sintering process has a large effect on the properties of the phase transformation. For the printed component, there is only one peak observed during heating and cooling, with no evidence of an intermediate R-phase. Furthermore, both peaks shift significantly to higher temperatures as described in the literature (Section 1.2). These effects of the selective laser sintering process on the phase transformation have been previously observed [40] (Figure 8) suggesting that there is a consistent effect from laser sintering Nitinol powder.

The cause of this shift to higher temperature has been hypothesized to be a number of different factors (Section 1.2). Saedi and coworkers suggested that the rise in transformation temperature was likely due to preferential evaporation of Ni during the 3D printing process [23, 49]. Dadbakhsh and coworkers outline several causes including residual stress within the part, the formation of precipitates involving Ni and Ti which shift the composition of Ni and Ti in the NiTi phase to higher Ni content, and the grain size of the components [40]. As the transformation temperatures of printed Nitinol are too high to be useful in medical devices for their superelastic properties, understanding the root cause behind the increase in transformation temperature for Nitinol is critical to making selective laser sintering a viable pathway to producing Nitinol components.

The effect of the laser sintering parameters on the printing process are shown in Figure 19 for a low, medium, and high power set of print parameters, each yielding reasonable relative density. The most evident difference between the transformation properties between these different print parameters is the nature of the transformation between martensite and austenite upon heating. The low and medium power settings show the two peak transformation that was found in the virgin powder, where the intermediate R-phase is formed, while the high power setting shows a single transformation peak. There is no clear trend in the transformation temperatures within the range of laser powers studied in this experiment. However, Dadbakhsh and coworkers have shown that at very high printing powers of 250 W, the shift in transformation temperatures is no longer present [40]. At this high of a power the part is being heated and cooled at a much faster rate than in the printing setup explored here, which provides an indication that reducing the amount of time that the component spends at high

temperatures can reduce and even effectively eliminate the shift in the transformation temperatures during printing.

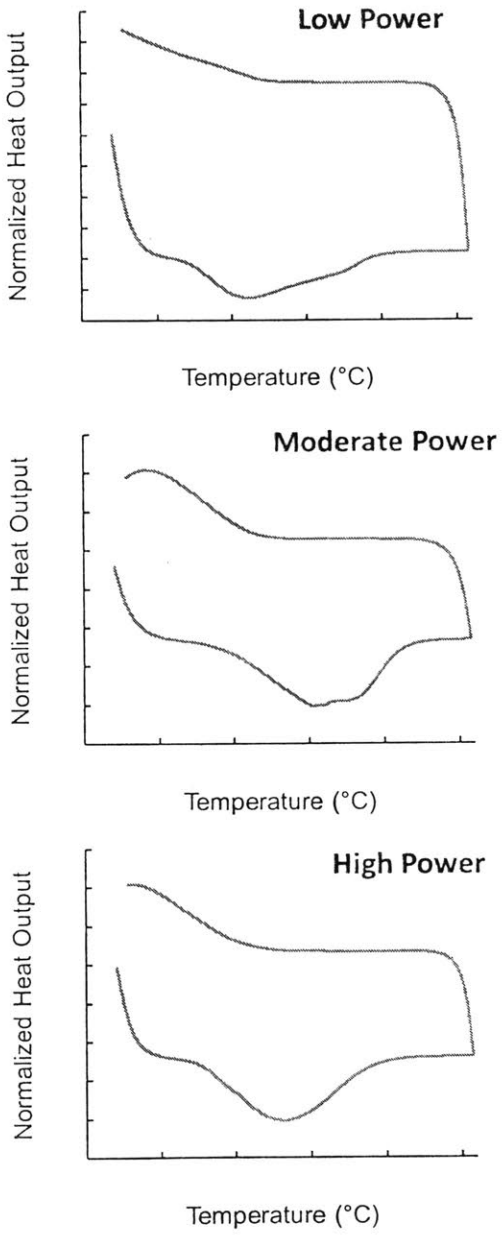

Figure 19. DSC of NiTi powder printed using different print parameters to study how the phase transformation is affected by the printing process.

Another processing route to tuning the transformation temperatures for printed Nitinol is to post-process the components through thermal annealing. Thermal annealing can affect the transformation temperatures in a few ways. First, thermal annealing can relieve residual stress built up in the components, which provides a barrier to the phase transformation. Evidence of residual stress in the part during printing was particularly clear under certain print conditions where parts delaminated during the printing process by curling up along the edges. Second, annealing can effect the internal microstructure of the printed components, for example by causing grain growth or by changing the phase composition of the component [40]. In particular, the changing of the phase composition by forming certain precipitates has been considered to be an important post-processing step in 3D printed Nitinol [36].

Figure 20 shows DSC curves for 3D printed Nitinol samples with different annealing recipes at moderate temperatures (450 to 500 °C) for 10 minutes. In each case, a single peak transformation is found both for the forward and reverse transformations. The sensitivity of the transformation temperatures to the annealing temperature is relatively small in the range of temperatures explored. An increase in the transformation temperatures from the as-printed samples of around 20 °C was measured, which is likely attributed to changes in the phase composition of the components (and likely the formation of oxides during annealing).

Further exploration of post-processing was conducted using vacuum annealing with a high pressure quench showing largely similar results. While the space of annealing procedures is quite large, the potential to decrease the transformation temperatures significantly through annealing is small based on these experiments and what has been found in the literature. More considered annealing studies have shown small decreases of the transformation temperatures during annealing of traditionally manufactured Nitinol, but not significant enough to be a viable path to reaching superelastic transformation temperatures in printed Nitinol components.

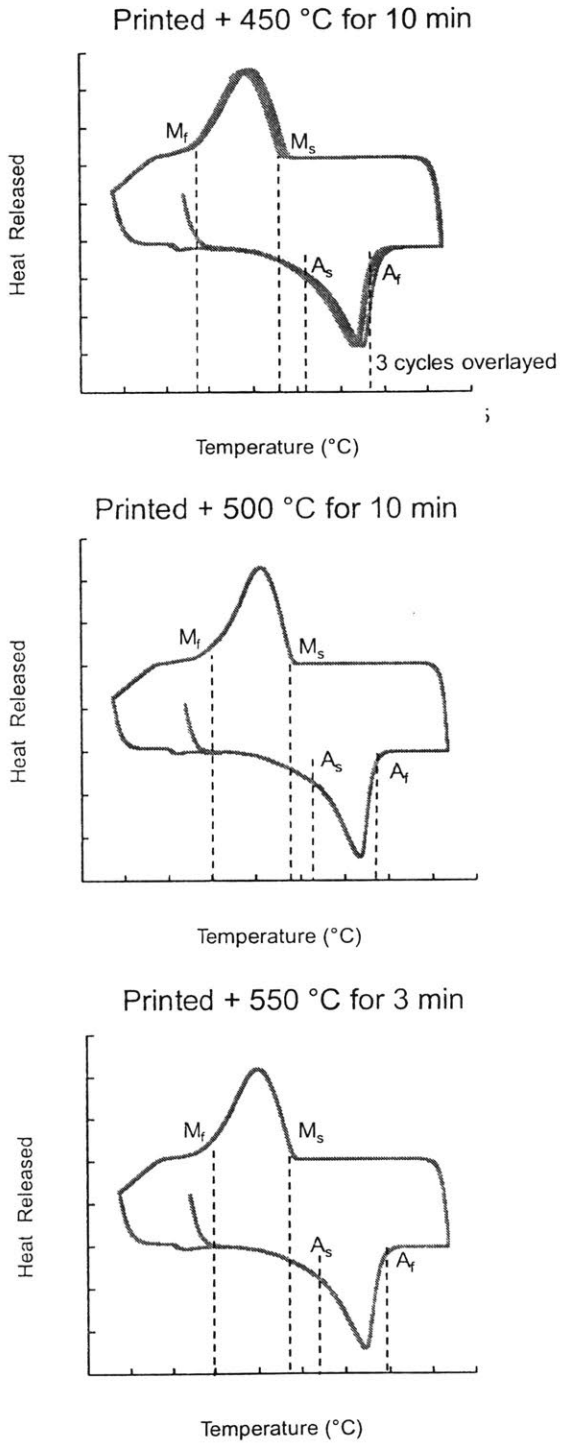

Figure 20. DSC of printed components with various post-annealing heat treatments

Haberland and coworkers suggested that the increase in the transformation temperatures during printing was due to Ni evaporation. The preferential loss of Ni is hypothesized to be due to the slightly higher melting/boiling points of Ti compared to Ni. When the Nitinol alloy is melted by the laser, the Ni is at a higher temperature relative to its boiling point and thus has a higher vapor pressure and likely a higher rate of evaporation. The potential for preferential Ni evaporation during selective laser sintering has been argued against because the difference in boiling points is not particularly high – 3560 K for Ti compared to 3186 K for Ni.

To detect any Ni loss during the printing process, chemical analysis by inductively coupled plasma mass spectrometry was conducted, using the same procedure and facilities, for the virgin Nitinol powder and the 3D printed Nitinol coupons. The chemical analysis showed a substantial loss of Ni during the selective laser sintering process, which was in line with the increase in the transformation temperature observed during 3D printing based on experiments showing the dependence of transformation temperatures on Ni content in Nitinol alloys [12]. While precise numbers for the amount of Ni content cannot be disclosed in this thesis, the difference in Ni content was able to explain the difference between the austenite finish temperatures of the Nitinol powder and the printed Nitinol component to within 5 °C.

The loss of Ni as the dominant reason for the increase in the transformation temperatures in printed Nitinol is also compatible with the other results found in this section. The lack of success from various heat treatments on the printed components suggests that the change in phase composition or grain structure is not a dominant factor, nor is the presence of residual stress. The larger effects observed from changing the printing power and speed on the other hand changes the amount of time the material spends in the melted state where preferential Ni loss is most significant, and success in the literature at eliminating the increase in transformation temperatures at very high speeds and powers suggests that if the time that the alloy spends in the heated/melted state is minimized the loss of Ni can be greatly decreased.

The use of a higher power laser thus seems to be one of the most viable routes to printing Nitinol. This option requires an investment in specialized selective laser sintering machines, which will be considered in Section 4. Another option is to account for the loss

of Ni by starting with Ni powder that is higher in Ni content. The relatively tight window of stability for Nitinol in the phase diagram limits the extent to which this can be done, but should be explored as Nitinol with up to 60 wt.% Ni has been produced in wrought ingots. The relatively limited supplier base for Nitinol makes sourcing higher Ni content powder a difficult option as well, and thus this option also requires significant investment.

The mass spectrometry of the powder and printed parts also revealed that the impurity content in the high quality Nitinol printed components were below ASTM F2063 maximum concentration standards [11], and only showed marginal increases relative to the impurity content of the powder. While the impurity contents meet the ASTM standards, it is generally desired to have impurity contents as low as possible, with internal standards at medical device companies often being stricter than the ASTM standards. As the majority of the impurity content is originally introduced in the Nitinol powder itself, improving gas atomization to limit the amount of impurities is an important area for future work.

In the next subsection, the mechanical properties of the printed Nitinol coupons are assessed at elevated temperatures to assess the current printed Nitinol alloys before discussing the remaining knowledge gaps for producing printed Nitinol alloys from an engineering and business perspective.

3.4.5 Analysis of the mechanical properties of printed Nitinol

Nitinol was printed into coupons as shown in Figure 21 based on a tensile specimen geometry provided specifically for metal 3D printed materials. The small size of these testing samples allow multiple samples to be printed in a single batch which allows for a higher throughput for testing. However, the small samples, particularly with the small amount of material around the pinholes, can lead to some deformation around the pinhole during testing, which can affect the interpretation of the final results.

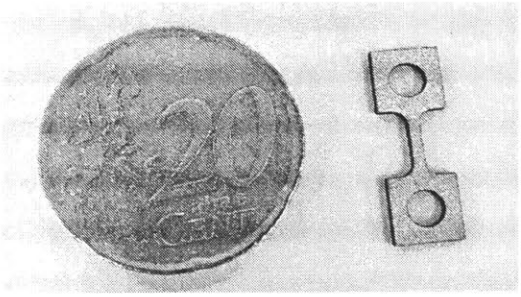

Figure 21. Geometry of tensile testing samples

Mechanical testing was performed on a high temperature Instron machine and held in place using rods through the pin-holes as shown in Figure 22. Sample holders were used to keep the specimen from moving out of the plane of testing. Sample holders were rigidly held in place in the Instron by tightening the screws shown in Figure 12 to minimize movement during the tensile test.

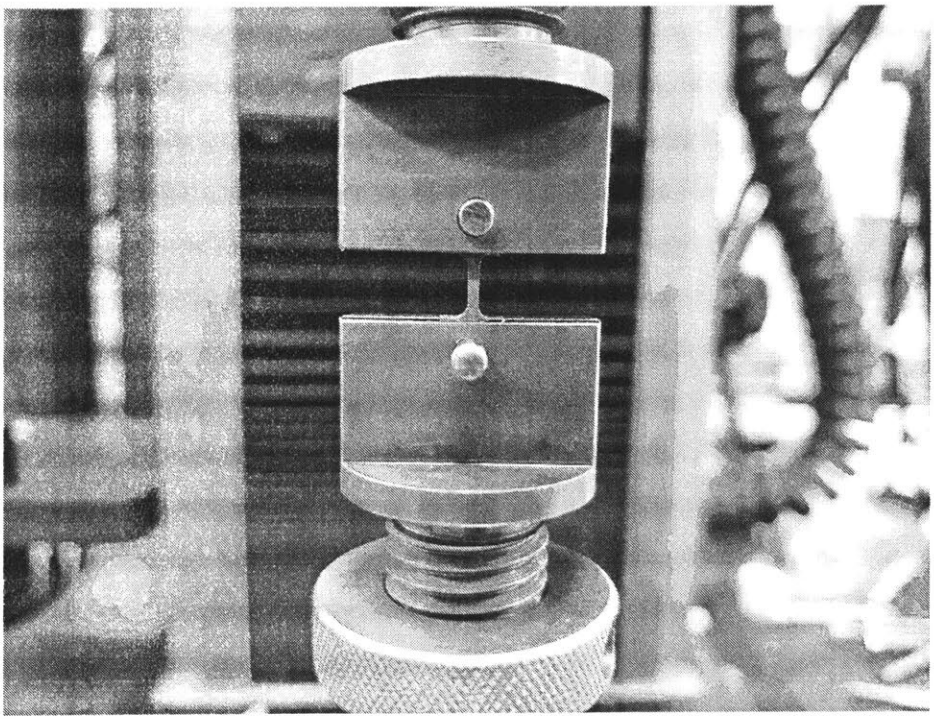

Figure 22. Mechanical testing experimental setup

The first type of tensile test conducted was to study the plastic deformation and fracture properties of the printed Nitinol. The sample was first elongated to a small strain and relaxed to observe any superelastic properties and then elongated to failure. Testing was conducted at both room temperature and elevated temperature (above the austenite finish temperature).

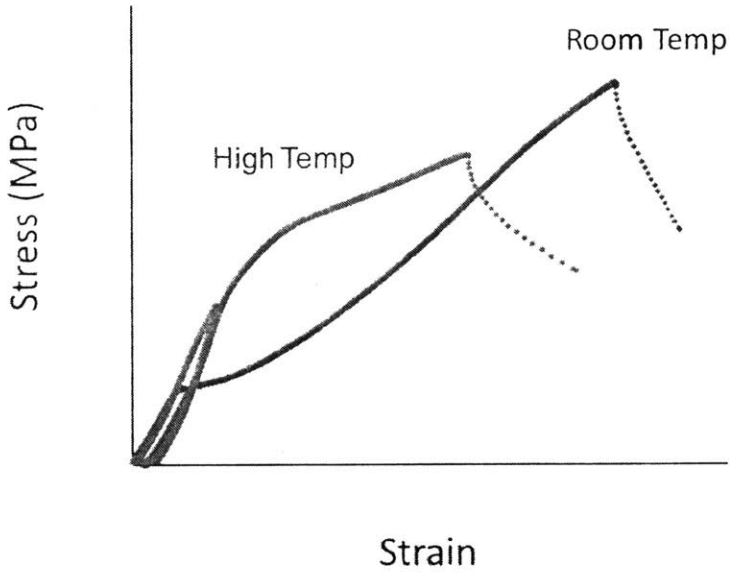

Figure 23. Stress-strain curves from tensile testing printed Nitinol samples, first cycling up to a fixed strain and then elongating to failure.

In both cases, no clear plateau was observed during elongation in the first cycle resembling superelasticity. When elongated to failure, a number of interesting properties of the printed Nitinol were observed (Figure 23):

1) The samples underwent plastic deformation and did not have a brittle fracture mode. This was a high importance performance metric in Table 2 and confirms that the high relative density and generally small pores present are sufficient to keep the part from failing in a brittle manner. Additionally, the presence of oxides or other inclusions are not leading to brittle fracture either, which confirms that the printing setup is able to produce high quality Nitinol parts with low impurity content. Of all samples tested, only samples that

underwent annealing as a post-processing step showed brittle failure, which can be explained by the increase in oxygen content and the formation of oxides.

2) The percent elongation of samples surpassed performance expectations based on traditionally manufactured Nitinol. This ductility is again made possible by the high relative density, low porosity, and low impurity content of the printed components, which support the feasibility of 3D printing Nitinol alloys.
3) The yield strength of components was within the range of suitable yield strength for a Nitinol alloy for medical devices. The yield strength was on the lower end of the desired range – as yield strength and percent elongation are often bounded by a trade-off between one another, this lower yield-strength is likely correlated to the higher percent elongation of the printed Nitinol.

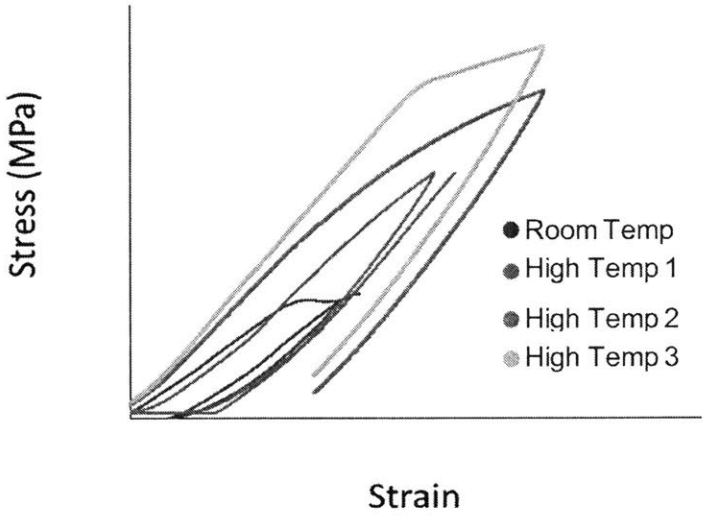

Figure 24. Stress-strain curves from cycling up to a fixed strain at several temperatures above the austenite finish temperature to study superelasticity.

The superelastic properties of Nitinol were tested at temperatures above the austenite finish temperature at various temperatures and under several different testing protocols. A summary of this tensile testing is presented in Figure 24 for different testing

temperatures. In samples exhibiting superelasticity, the samples should return to near zero strain after a strain cycle like the one conducted. In this study, none of the samples tested showed strong superelasticity. This is somewhat of a surprise given that all of these samples showed a clear phase transformation under a thermal cycle.

There are a number of reasons that could be contributing to the lack of superelasticity in these samples. First, the samples are not at the desired Ni to Ti ratio, which may affect the ease with which the martensite to austenite phase transformation can occur reversibly. To test this hypothesis, samples were held at a constant tensile load and the temperature was ramped from 0 °C until the samples showed a completed phase transformation. The temperature at which the transformation finished, i.e. the austenite finish temperature (at a constant load) was recorded for several loads ranging from 0 to 500 MPa. A sample exhibiting normal stress-induced phase transformation in Nitinol would generally show a linear and significant change in the austenite finish temperature with increasing stress, as described by the Clausius-Clapeyron relationship. However, the samples tested showed no consistent change in the austenite finish temperature, which suggests that the loss of Ni could be contributing to the difficulty in observing a phase transformation. Second, the samples themselves, due to their small size, may be leading to substantial experimental error. In Figure 24, the samples each show a substantially different slope in the elastic regime when the Young's modulus for all of the samples considered should be the same. The onset of plastic deformation was also highly varied between the different samples tested. Since this type of inconsistency was not present in the DSC experiments, it is possible that the test setup itself contributed a large testing error which obfuscated the presence of any superelastic effect present. Finally, it is interesting to note that testing of superelasticity of 3D printed Nitinol in the literature has been by and large compressive testing as opposed to the tensile testing that was performed in this study. Future testing of Nitinol 3D printed components will involve using new protocols for testing to reduce the variation induced from the testing setup and ensure more consistent results.

The shape memory properties of printed Nitinol were not quantitatively tested, as no immediate applications for these properties were under consideration. However, the high austenite finish temperatures of the printed parts naturally lend themselves to shape

memory applications. Shape memory was tested by bending tensile bars to a 45 degree angle at room temperature and placing them in a furnace above the austenite finish temperature. Components showed almost full recovery to the as-printed shape of the tensile bar.

3.4.6 Summary of feasibility assessment for 3D printing Nitinol

In this section, the feasibility of 3D printing Nitinol with the necessary engineering properties to be useful in medical devices was assessed by performing experiments to determine 1) whether printing parameters could be readily developed to create components with desired microstructure and chemical properties, and 2) if the microstructure and chemical properties could be controlled well enough to produce desired mechanical properties such as good ductility and superelasticity. In exploring the space of printing parameters to produce low defect Nitinol parts, it was found that a range of printing parameters could produce parts with low porosity, which was in-line with findings in the literature. However, these components were found to have higher-than-desired transformation temperatures, which prohibited their usefulness at body temperature where superelasticity was required. This increase in the transformation temperatures due to the printing process was found to be due to the preferential evaporation of Ni during printing, leading to a lower Ni concentration in the final components. When samples were mechanical tested in the austenite state, they showed good ductility, with % elongations surpassing the specifications for Nitinol. However, superelasticity was not observed in early testing, which could be attributed to both the need for more refined testing procedures to observe superelasticity as well as the loss of Ni potentially affecting the ability of the components to undergo a stress-induced phase transformation reversibly.

In the next section, these experimental results are combined with an operational and business assessment to provide a holistic view of the potential of 3D printed Nitinol and identify the most relevant categories of Nitinol components for 3D printing.

4. Assessment of Opportunities for Producing Quality Nitinol Components

4.1 Identifying best attributes and biggest risks for 3D printed Nitinol based on the engineering assessment

The experiments conducted in Section 3.4. provided valuable preliminary data aimed to meet the engineering specifications described in Table 2. Table 5 provides a risk level for meeting these engineering specifications based on the characterization of printed Nitinol parts that was conducted.

Among mechanical properties, the experiments provided confidence in being able to meet the yield strength and % elongation at failure. However, the high transformation temperatures and the loss of Ni made it difficult to produce superelastic Nitinol. In addition, meeting tight dimensional tolerances remains a challenge even after electropolishing components. These observations will inform the target applications identified later in this section.

Table 5. Risk assessment of achieving engineering properties of Nitinol based on experimental analysis

Property	Risk Level:	Importance to Stakeholders
Yield strength	*Low*	*High*
% elongation at failure	*Low*	*High*
% plastic strain after recovery	*High*	*High*
Upper plateau strength	*Moderate*	*Moderate*
Lower plateau strength	*Moderate*	*Moderate*
Ultimate tensile strength	*Low*	*Low*
Young's modulus	*Low*	*Low*
Shape memory effect extent	*Moderate*	*Low*
# of cycles to failure	*High*	*High*
Dimensional tolerances	*High*	*High*
Corrosion resistance	*Not evaluated*	*High*
Biocompatibility	*Not evaluated*	*High*

Based on the experimental findings, the importance of different process parameters for future development of Nitinol selective laser sintering are summarized in Table 6. To address the difficulties in attaining superelasticity, the critical process parameters for further control are the Nitinol powder chemistry and the printing process parameters. Nitinol powder chemistry includes both increasing the Ni content to offset the loss of Ni during sintering as well as reducing the amount of impurities in the powder which have a large influence on the impurity content of the final components. Within the printing process parameters, operating at higher laser powers and scan speeds could help reduce the amount of Ni evaporation and produce superelastic Nitinol components.

Table 6. Weighting key tunable additive process parameters in terms of importance to achieving desired Nitinol properties

Process Parameter	Process Phase	Importance for Optimization
Nitinol powder size & shape	*Raw Material*	*Moderate*
Nitinol powder chemistry	*Raw Material*	*High*
Laser power	*Printing*	*High*
Laser scan speed	*Printing*	*High*
Laser scan pattern	*Printing*	*Moderate*
Layer thickness	*Printing*	*Moderate*
Support structures	*Printing*	*Moderate*
Solution annealing	*Post Processing*	*Moderate-High*
Electropolishing	*Post Processing*	*Low*
EDM wiring	*Post Processing*	*Low*

4.2 Applications to target based on engineering feasibility analysis

In considering Nitinol applications broadly, three attributes of Nitinol are useful or potentially useful in medical devices: superelasticity, shape memory, and ductility (Section 1.1.2). To date, superelasticity is by far the most utilized attribute of Nitinol in the medical device industry [9]. However, the ability to make components directly to their net shape instead of building from Nitinol wire enables the use of Nitinol in new ways.

Based on the engineering feasibility assessment, ductile Nitinol is the most clearly viable application of 3D printing currently. Components consistently exhibited good % elongation to failure and elasticity without brittle fracture. Superelasticity was not observed in the printed components, and thus while the current uses of superelastic components are the most numerous, there remain significant engineering challenges to address before this type of application can be pursued. Shape memory applications are another promising case based on the engineering assessment as components exhibited shape memory and naturally have transformation temperatures compatible with good shape memory properties.

There are three types of ways in which 3D printing can be used for Nitinol devices: prototyping, manufacturing existing components, and enabling manufacturing of new components. Applications fall into 9 categories based on the property of Nitinol that is critical for the product and the type of opportunity to apply 3D printing, as shown in Figure 25.

	Prototyping	Existing Parts	New Parts
Superelastic		Stents, Guidewires	Bulk components
Shape Memory		Actuators	Bulk components
Ductility		Select stents	Porous parts, Mechanical compatability

Figure 25. Categories of applications for Nitinol 3D printed components

Developing 3D printed Nitinol components to replace existing Nitinol components is a challenging task. Current Nitinol components are designed to be constructed with traditional Nitinol manufacturing techniques. As a result, designs assume that Nitinol can only be provided in a wire or tube form and thus the types of shapes that can be made are limited. Furthermore, traditional applications such as stents have very thin struts which could be difficult to achieve based on the surface roughness

and limited resolution of selective laser sintering (Section 3). In addition, as most current applications use the superelastic properties of Nitinol, significant work remains to demonstrate that quality components can be made from an engineering standpoint and to de-risk the use of this technology for implants. Based on the engineering assessment, the use of selective laser sintering for existing Nitinol components is only reasonable in the long-term and requires significant research milestones to be met.

Prototyping applications on the other hand are aimed to help the product development process by producing new designs at low volume and reasonably low cost. The readily demonstrated ductility and shape memory properties of the printed Nitinol show immediate promise for prototyping applications. The engineering assessment also showed that superelasticity could be expected through future work using higher laser power printers, new powder, etc., which could give product development teams a new way to test complex geometries and designs for Nitinol components. As prototyping applications do not need to meet the same rigorous quality standards of medical devices, it is reasonable to expect Nitinol to be printed for these applications in the short-term.

Perhaps the most promising set of applications is newly designed Nitinol components. Two types of newly designed Nitinol components can be imagined. First, 3D printing enables the development of new geometries for existing Nitinol parts. Instead of trying to adapt 3D printing to replicate existing Nitinol component geometries, there are opportunities to develop higher performance components that can be more easily manufactured by 3D printing [53]. However, this again requires substantial investment and risk-taking from product development teams to develop and test such designs when strong alternatives using traditional manufacturing exist.

The second type of newly designed component is 3D printed Nitinol that either adds performance by replacing a component made of a different material or enables an entirely new medical device. 3D printing Nitinol enables the production of "bulk" Nitinol parts – i.e. parts that are not fundamentally formed by wire or tube. For instance, a a shape memory Nitinol component can enable external actuation in an implant to eliminate multiple surgeries to change out material (Section 1.1.2). Often assemblies of parts benefit from contact of like materials, and there is demand for bulk Nitinol components to be matched with other Nitinol parts in existing medical devices, replacing

titanium, steel, etc. New components utilizing the ductility of Nitinol can also be designed with lattice or porous structures (Figure 26 [34]) which can be used as scaffolds, to match the mechanical stiffness of bone, or reduce the amount of material in a part [42]. In this set of applications, 3D printed Nitinol provides a substantial performance advantage which makes a stronger case for investing in the development of the technology given the engineering risks of printing commercial medical device parts.

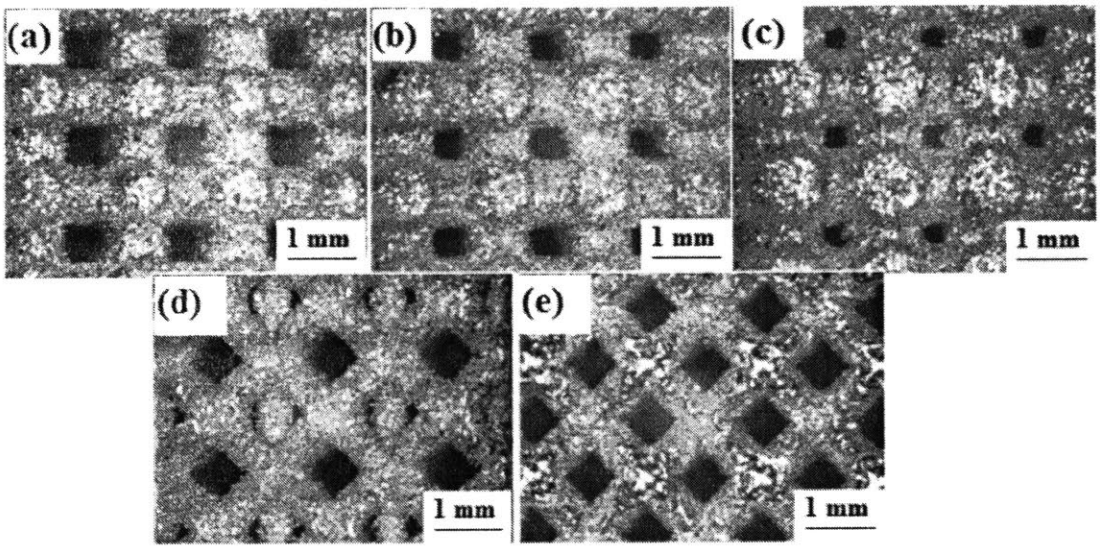

Figure 26. Several types of lattice/porous Nitinol components (a-e) that could provide performance advantages over existing components (reproduced with permission from Andani et. al. [34]).

The engineering assessment provides support for printing components for prototyping efforts and for developing entirely new Nitinol components as these can be accomplished in the short-terma nd provide substantial value to the medical device industry through higher performance devices and shorter design times. To better understand the costs associated with manufacturing Nitinol components using selective laser sintering to further select the particular types of components that are most ripe for implementing this technology, a cost accounting model is presented in the next section.

4.3. A cost accounting model for selective laser sintering of Nitinol

The cost accounting model for selective laser sintering of Nitinol was developed based on the generalized selective laser sintering model proposed by Rickenbacher et. al. [54]. The model breaks down the costs of selective laser sintering into the different phases of the printing process and calculates costs in each phase including material, labor, equipment costs, etc. Figure 27 shows the cost accounting model breakdown schematically.

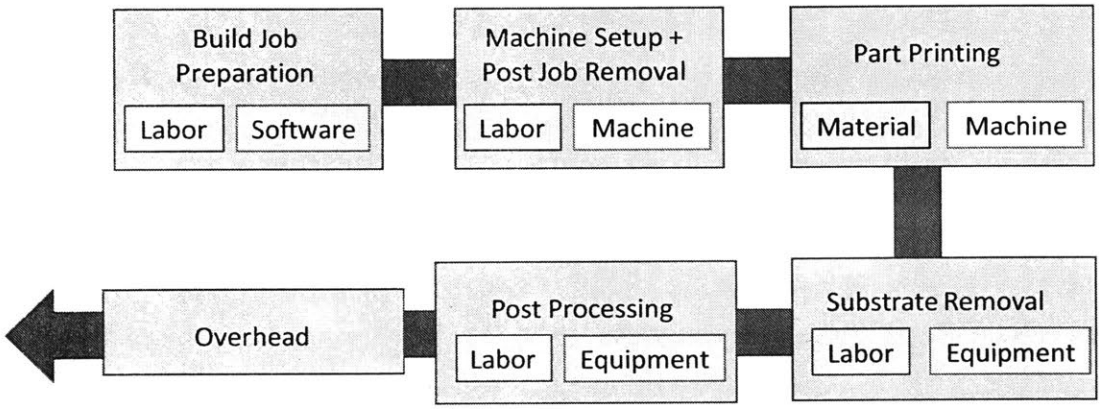

Figure 27. Modular view of the cost accounting model for Nitinol additive manufacturing

The first step in the selective laser sintering process is preparing the digital part file, or CAD file, from which the machine will print the component. Preparation of the part file requires a trained engineer with knowledge of how to design for additive manufacturing to make any adaptations necessarily to ensure that the part is printable. In addition to this labor cost (engineer salary per hour * time), the software packages require licenses which can be attributed to an individual project by dividing by the total number of projects in a year.

The machine needs to be setup before running the job with the proper powder (in this case Nitinol), which may mean removing a different type of powder from the machine and cleaning. In addition to the labor cost, the time to setup the machine also uses up possible operational time for the machine, and thus the hourly cost of the machine must also be accounted for. Similar costs are associated with removing the component.

During printing, the machine cost is calculated based on the print job time. The time that it takes to print the job depends strongly on the part geometry. Parts with a larger printing height take longer times to build as more layers need to be printed. The model for determining the time a part will take to print from part geometry can be developed using a linear regression model [54]. The Nitinol powder is consumed during the printing in a few ways. Nitinol that is printed into the component needs to be accounted for (using the part volume). In addition, some Nitinol powder near the printed component becomes heated and some loosely melted parts will conglomerate near the component as well. The loss of powder from a batch depends on how much powder is reused, if any. In the present model, no reuse of powder is assumed as it is unclear for Nitinol to what extent the adjacent powder in the bed is affected by heat and whether filtering away larger particles through a sieve is sufficient for powder reuse. Testing for reusability of powder and developing safe protocols for doing so could greatly reduce costs of Nitinol selective laser sintering.

Once the part is printed and removed from the machine, the part needs to be removed from the substrate. Costs for this vary based on whether the component is removed with an EDM wire (necessary for production components) or removed manually (more likely for prototyping and much cheaper).

Nitinol carries specific costs related to post-processing to achieve the desired surface finish and transformation properties. Electropolishing is included for all components considered in this model as it is likely worthwhile for both prototyping and production components. Heat treating may be necessary for certain applications, for instance to set a certain shape in the Nitinol part for a shape memory application.

Lastly, overhead costs for selective laser sintering can be quite substantial. There is traditional overhead such as lab space, maintenance, etc., but in this model overhead also accounts for research and development costs which ultimately dominate the overhead for Nitinol selective laser sintering. For Nitinol to be printed, there are substantial risks that a particular build can fail as it is a relatively new material without fully-vetted protocols for dimensional tolerances, overhangs, and other geometrical limitations. In this model overhead is included as a percentage of the total cost of the part.

4.4. Identifying best attributes and biggest risks for 3D printed Nitinol based on the cost accounting model

The cost model was used to understand the main cost drivers for Nitinol 3D printing. Figure 28 shows the main cost drivers for printing Nitinol as a function of part size and part volume. For this exercise, small components are defined as components for which 25 to 75 components could fit on a standard build plate (roughly a 10 cm by 10 cm square) as opposed to only 1-10 components for a large component. Prototyping builds can often be ordered for low volumes where a full build plate is not used, which is denoted as low volume in Figure 28, whereas in production the full build plate would be used (high volume). The y-axis of cost is scaled consistently across the different graphs in Figures 28 and 29.

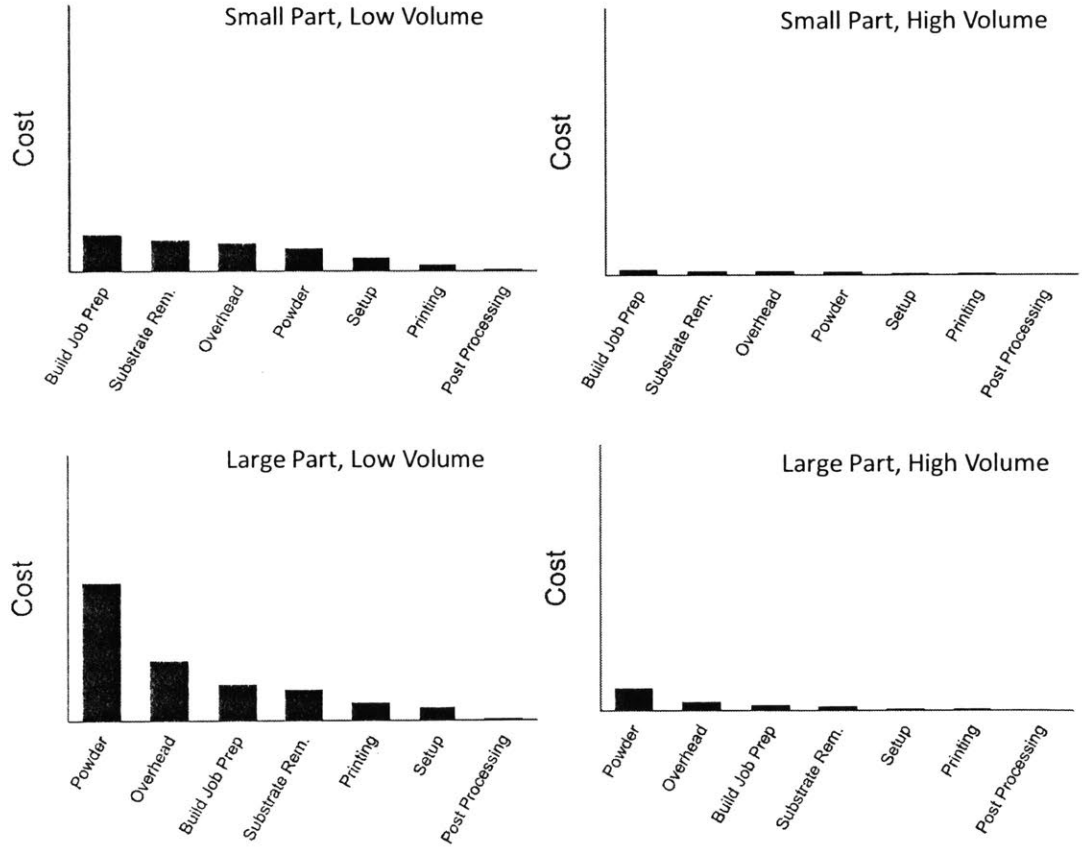

Figure 28. Case studies using the cost accounting model for small and large parts and small and large volumes.

The dominant cost drivers depend strongly on the size of the part being printed and are virtually independent of the volume of parts. For small parts, the printing costs are all relatively small, including the costs of the machine time and the Nitinol powder. The dominant costs are related to labor of skilled engineers, which is why preparing the build job, overhead, and substrate removal are the dominant cost drivers. For large parts, the dominant cost is powder. Nitinol powder is relatively expensive (about 1.5 to 3 times the cost of titanium or stainless steel powders) and printing large Nitinol components also leads to a lot of wasted powder in the powder bed that isn't used.

Based on these results, selective laser sintering of relatively small components (millimeter scale) is very cost effective. Considering that the dominant costs are labor related, and selective laser sintering is substantially less labor intensive than traditional Nitinol manufacturing, selective laser sintering is expected to generate significant cost savings for smaller components relative to traditional methods. This niche for selective laser sintering is particularly significant as smaller components are generally the most expensive to manufacture using conventional methods (e.g. micromachining), and many medical device components fall into this category.

On the other hand, printing large components is unlikely to be favorable from a cost perspective due to the dominant cost of powder. Powder costs are higher than normal material costs for traditional manufacturing and, whereas in many additive manufacturing applications the amount of waste material is less than traditional manufacturing, in this case the amount of waste material in the powder bed is significant. In addition, Nitinol powder is supplied by very few companies and produced in small batches. Printing large components with current supply lead times (up to 6 months for 50 to 100 kg) would require substantial powder inventory be held, which would increase costs as well.

A second case study was performed using the cost accounting model to determine the main costs in the scenario of investing in a printer with higher laser power to develop superelastic Nitinol in the as-printed state. Figure 29 shows the cost breakdown for high laser power printing, which can also be interpreted as any type of specialized printing for Nitinol, e.g. high resolution printers.

In the scenario of a high cost, specialized printer for Nitinol, the costs are substantially higher for low volume builds compared to high volume builds. Using a

specialized printer for only prototyping builds, with a few parts per printing run, would be highly ineffective and likely unfeasible from a cost perspective. On the other hand, the high volume builds compare reasonably cost-wise with the conventional printer costs in Figure 28, which means that a specialized printer would be cost-effective for production applications but not for prototyping operations. In all cases, the dominant cost of printing is the cost of the printer itself which reduces the impact of part size on costs for powder reasons. However, taller parts take a longer amount of time to print per component and will have substantially higher costs as a result, which again benefits the use of this technology for smaller components (a few millimeters in size).

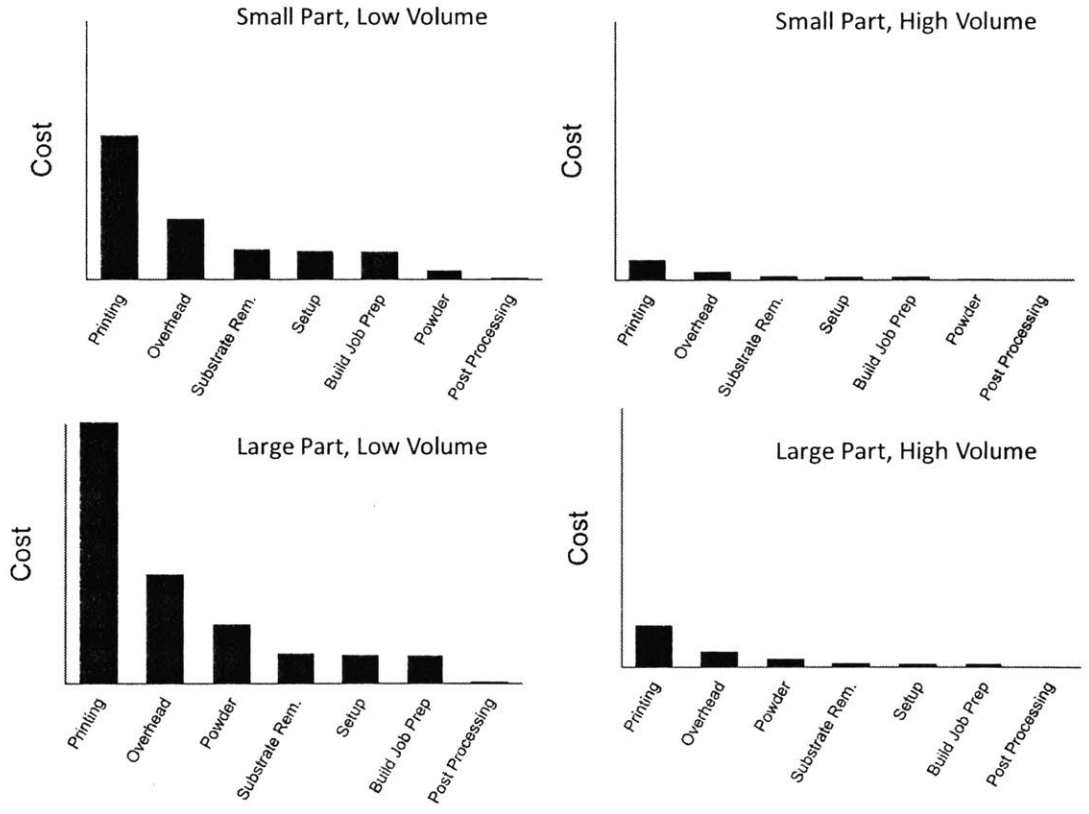

Figure 29. Case studies using the cost accounting model for high laser power, specialized printing.

4.5 Summary of opportunity assessment for Nitinol 3D printed medical devices

Figure 30 revisits the breakdown from the beginning of this section where the potential applications for Nitinol were categorized based on the Nitinol property needed for the application and the type of printing opportunity.

Based on the engineering analysis, the applications relying on Nitinol's ductility and shape memory properties are most likely to succeed in the short-term, as opposed to superelasticity which requires further research. In addition, the limitations in surface treatment and dimensional tolerance lends itself to prototyping applications or to new Nitinol parts that are designed with these limitations in mind with the intent of exploiting the strengths of 3D printing to produce novel components (e.g. lattice structures or bulk Nitinol parts).

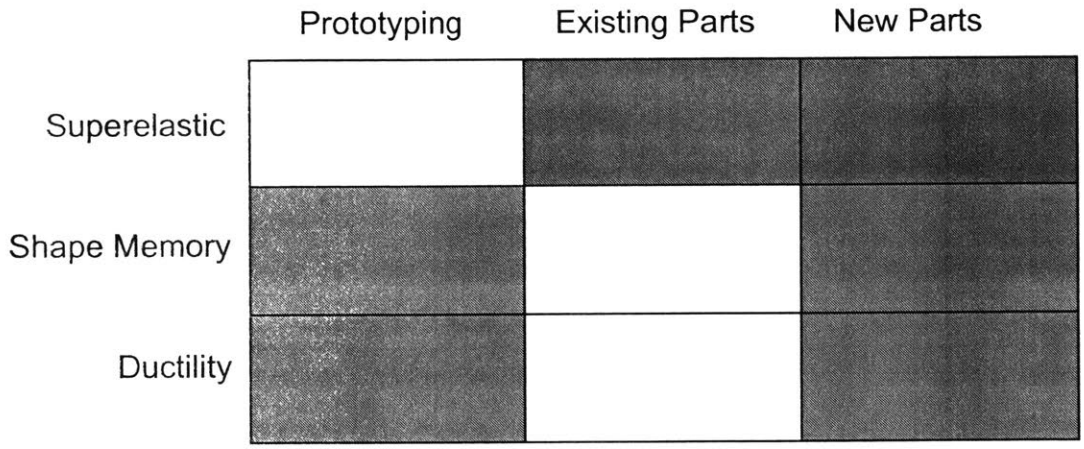

Figure 30. Nitinol applications evaluated based on the engineering analysis and cost accounting model (green – feasible in the short term, yellow – feasible with 1-2 years of research, red – requires substantial research and investment).

The cost accounting model revealed that, when using a standard commercial printer, both prototyping and production parts could lead to significant cost savings over traditional manufacturing for small components (on the scale of a few millimeters). The dominant cost for small components was engineering labor, which is expected to be substantially lower than labor costs for traditional manufacturing of components of this size. Prototyping costs were larger for specialized printers that could enable printing

Nitinol in a superelastic form compared to production builds which would more judiciously use build plate real estate.

Based on these analyses, the most likely short-term applications of Nitinol will be in prototyping and the development of new components that are a few millimeters in size that utilize the good ductility of Nitinol and/or its shape memory property. Further research is required for developing superelastic Nitinol, which will enable an additional wave of applications with a 1 to 2-year investment.

5. Conclusions

3D printing of Nitinol using selective laser sintering is an exciting technology with the potential to reduce the costs and time of manufacturing Nitinol components in medical devices. In this thesis, the opportunities for using selective laser sintering for Nitinol are identified first from an engineering perspective, considering the range of properties that are achievable and the current limitations and risks of implementing this technology. This engineering analysis is combined with a business case analysis considering applications of Nitinol 3D printed parts for prototyping, replacing existing Nitinol components, and developing entirely new products which includes consideration for the size and volume of components using a cost accounting model specifically for Nitinol selective laser sintering. The main findings from this analysis are:

1) Nitinol components with low porosity and low impurity contents, satisfying medical device standards for high quality Nitinol, can be readily printed using commercial selective laser sintering printers using a design of experiment optimization.
2) Surface roughness of Nitinol 3D printed components can be treated using electropolishing to remove most asperities from the surface and reduce the chance of brittle failure.
3) The process of laser melting leads to preferential evaporation of Ni, which increases the austenite finish temperature from the powder to the printed Nitinol component. This brings the austenite finish temperature out of the range for superelastic applications of Nitinol
4) Nitinol components showed good ductility and shape memory properties in mechanical testing, but poor superelasticity due to the loss of Ni.
5) Selective laser sintering of Nitinol is most directly useful for prototyping and the production of entirely new Nitinol component designs where the trade-offs between the cost of investment and the benefits of implanting the technology are well-aligned.
6) The cost accounting model of selective laser sintering of Nitinol shows a strong preference for producing smaller components, where labor dominates the costs and selective laser sintering should be favorable to traditional manufacturing.

6. References

[1] Conner, B. P., Manogharan, G. P., Martof, A. N., Rodomsky, L. M., Rodomsky, C. M., Jordan, D. C., & Limperos, J. W. (2014). Making sense of 3-D printing: Creating a map of additive manufacturing products and services. *Additive Manufacturing*, *1*, 64-76.

[2] Attaran, M. (2017). The rise of 3-D printing: The advantages of additive manufacturing over traditional manufacturing. *Business Horizons*, *60*(5), 677-688.

[3] Ford, S. L. (2014). Additive manufacturing technology: potential implications for US manufacturing competitiveness. *J. Int'l Com*

[4] Wohlers, T., Campbell, I., & Diegel, O. (2018). Wohlers Report 2018. *Fort Collins: Wohlers Associates*.

[5] Frazier, W. E. (2014). Metal additive manufacturing: a review. *Journal of Materials Engineering and Performance*, *23*(6), 1917-1928.

[6] Lewandowski, J. J., & Seifi, M. (2016). Metal additive manufacturing: a review of mechanical properties. *Annual Review of Materials Research*, *46*, 151-186.

[7] Sames, W. J., List, F. A., Pannala, S., Dehoff, R. R., & Babu, S. S. (2016). The metallurgy and processing science of metal additive manufacturing. *International Materials Reviews*, *61*(5), 315-360.

[8] Duerig, T. W., Pelton, A., & Stöckel, D. (1999). An overview of nitinol medical applications. *Materials Science and Engineering: A*, *273*, 149-160.

[9] Morgan, N. B. (2004). Medical shape memory alloy applications—the market and its products. *Materials Science and Engineering: A*, *378*(1-2), 16-23.

[10] Pelton, A. R., Dicello, J., & Miyazaki, S. (2000). Optimisation of processing and properties of medical grade Nitinol wire. *Minimally Invasive Therapy & Allied Technologies*, *9*(2), 107-118. [11] ASTM F2063-05 (American Society for Testing Materials, 2005).

[12] Frenzel, J., George, E. P., Dlouhy, A., Somsen, C., Wagner, M. X., & Eggeler, G. (2010). Influence of Ni on martensitic phase transformations in NiTi shape memory alloys. *Acta Materialia*, *58*(9), 3444-3458.

[13] Elahinia, M., Moghaddam, N. S., Andani, M. T., Amerinatanzi, A., Bimber, B. A., & Hamilton, R. F. (2016). Fabrication of NiTi through additive manufacturing: A review. *Progress in Materials Science*, *83*, 630-663.

[14] Wu, M. H. (2002). Fabrication of nitinol materials and components. In *Materials Science Forum* (Vol. 394, pp. 285-292). Trans Tech Publications.

[15] Elahinia, M. H., Hashemi, M., Tabesh, M., & Bhaduri, S. B. (2012). Manufacturing and processing of NiTi implants: A review. *Progress in materials science*, *57*(5), 911-946.

[16] Mentz, J., Bram, M., Buchkremer, H. P., & Stöver, D. (2006). Improvement of mechanical properties of powder metallurgical NiTi shape memory alloys. *Advanced engineering materials*, *8*(4), 247-252.

[17] Penrod, L. E. (2004). *Fabrication and characterization of porous shape memory alloys* (Doctoral dissertation, Texas A&M University).

[18] Bansiddhi, A., Sargeant, T. D., Stupp, S. I., & Dunand, D. C. (2008). Porous NiTi for bone implants: a review. *Acta biomaterialia*, *4*(4), 773-782.

[19] Cheng, B., Shrestha, S., Chou, K., (2016). Stress and deformation evaluations of scanning strategy effect on selective laser melting. *Additive Manufacturing*, 12(B), 240-251.

[20] Meier, H., Haberland, C., & Frenzel, J. (2011). Structural and functional properties of NiTi shape memory alloys produced by selective laser melting. *Innovative developments in design and manufacturing: advanced research in virtual and rapid prototyping*, 291-296.

[21] Meier, H., & Haberland, C. (2008). Experimental studies on selective laser melting of metallic parts. *Materialwissenschaft und Werkstofftechnik*, *39*(9), 665-670.

[22] Meier, H., Haberland, C., Frenzel, J., & Zarnetta, R. (2009). Selective Laser Melting of NiTi shape memory components. In *Innovative Developments in Design and Manufacturing* (pp. 251-256). CRC Press.

[23] Haberland, C., Elahinia, M., Walker, J. M., Meier, H., & Frenzel, J. (2014). On the development of high quality NiTi shape memory and pseudoelastic parts by additive manufacturing. *Smart materials and structures*, *23*(10), 104002.

[24] Haberland, C., Meier, H., & Frenzel, J. (2012, September). On the properties of Ni-rich NiTi shape memory parts produced by selective laser melting. In *ASME 2012 conference on smart materials, adaptive structures and intelligent systems* (pp. 97-104). American Society of Mechanical Engineers.

[25] Haberland, C., Elahinia, M., Walker, J., Meier, H., & Frenzel, J. (2013, September). Additive manufacturing of shape memory devices and pseudoelastic components. In *ASME 2013 conference on smart materials, adaptive structures and intelligent systems* (pp. V001T01A005-V001T01A005). American Society of Mechanical Engineers.

[26] Haberland, C., Elahinia, M., Walker, J., & Meier, H. (2013, September). Visions, concepts and strategies for smart nitinol actuators and complex nitinol structures produced by additive manufacturing. In *ASME 2013 Conference on Smart Materials, Adaptive Structures and Intelligent Systems* (pp. V001T01A006-V001T01A006). American Society of Mechanical Engineers.

[27] Walker, J. M. (2014). Additive manufacturing towards the realization of porous and stiffness-tailored NiTi implants.

[28] Walker, J., Elahinia, M., & Haberland, C. (2013, September). An investigation of process parameters on selective laser melting of nitinol. In *ASME 2013 Conference on Smart Materials, Adaptive Structures and Intelligent Systems* (pp. V001T01A007-V001T01A007). American Society of Mechanical Engineers.

[29] Walker, J. M., Haberland, C., Taheri Andani, M., Karaca, H. E., Dean, D., & Elahinia, M. (2016). Process development and characterization of additively manufactured nickel–titanium shape memory parts. *Journal of Intelligent Material Systems and Structures*, *27*(19), 2653-2660.

[30] Taheri Andani, M. (2015). *Modeling, Simulation, Additive Manufacturing, and Experimental Evaluation of Solid and Porous NiTi* (Doctoral dissertation, University of Toledo).

[31] Saedi, S., Turabi, A. S., Andani, M. T., Haberland, C., Karaca, H., & Elahinia, M. (2016). The influence of heat treatment on the thermomechanical response of Ni-rich NiTi alloys manufactured by selective laser melting. *Journal of Alloys and Compounds*, *677*, 204-210.

[32] Saedi, S., Turabi, A. S., Andani, M. T., Haberland, C., Elahinia, M., & Karaca, H. (2016). Thermomechanical characterization of Ni-rich NiTi fabricated by selective laser melting. *Smart Materials and Structures*, *25*(3), 035005.

[33] Saedi, S., Turabi, A. S., Andani, M. T., Moghaddam, N. S., Elahinia, M., & Karaca, H. E. (2017). Texture, aging, and superelasticity of selective laser melting fabricated Ni-rich NiTi alloys. *Materials Science and Engineering: A*, *686*, 1-10.

[34] Andani, M. T., Saedi, S., Turabi, A. S., Karamooz, M. R., Haberland, C., Karaca, H. E., & Elahinia, M. (2017). Mechanical and shape memory properties of porous Ni50. 1Ti49. 9 alloys manufactured by selective laser melting. *Journal of the mechanical behavior of biomedical materials*, *68*, 224-231.

[35] Taheri Andani, M., Haberland, C., Walker, J. M., Karamooz, M., Sadi Turabi, A., Saedi, S., & Elahinia, M. (2016). Achieving biocompatible stiffness in NiTi through additive manufacturing. *Journal of Intelligent Material Systems and Structures*, *27*(19), 2661-2671.

[36] Saedi, S., Moghaddam, N. S., Amerinatanzi, A., Elahinia, M., & Karaca, H. E. (2018). On the effects of selective laser melting process parameters on microstructure and thermomechanical response of Ni-rich NiTi. *Acta Materialia*, *144*, 552-560.

[37] Ma, C., Andani, M. T., Qin, H., Moghaddam, N. S., Ibrahim, H., Jahadakbar, A., ... & Dong, Y. (2017). Improving surface finish and wear resistance of additive manufactured nickel-titanium by ultrasonic nano-crystal surface modification. *Journal of Materials Processing Technology*, *249*, 433-440.

[38] Khoo, Z., Liu, Y., An, J., Chua, C., Shen, Y., & Kuo, C. (2018). A review of selective laser melted NiTi shape memory alloy. *Materials*, *11*(4), 519.

[39] Dadbakhsh, S., Speirs, M., Kruth, J. P., & Van Humbeeck, J. (2015). Influence of SLM on shape memory and compression behaviour of NiTi scaffolds. *CIRP Annals*, *64*(1), 209-212.

[40] Dadbakhsh, S., Speirs, M., Kruth, J. P., Schrooten, J., Luyten, J., & Van Humbeeck, J. (2014). Effect of SLM parameters on transformation temperatures of shape memory nickel titanium parts. *Advanced Engineering Materials*, *16*(9), 1140-1146.

[41] Dadbakhsh, S., Vrancken, B., Kruth, J. P., Luyten, J., & Van Humbeeck, J. (2016). Texture and anisotropy in selective laser melting of NiTi alloy. *Materials Science and Engineering: A, 650*, 225-232.

[42] Dadbakhsh, S., Speirs, M., Van Humbeeck, J., & Kruth, J. P. (2016). Laser additive manufacturing of bulk and porous shape-memory NiTi alloys: From processes to potential biomedical applications. *MRS Bulletin, 41*(10), 765-774.

[43] Speirs, M., Van Hooreweder, B., Van Humbeeck, J., & Kruth, J. P. (2017). Fatigue behaviour of NiTi shape memory alloy scaffolds produced by SLM, a unit cell design comparison. *Journal of the mechanical behavior of biomedical materials, 70*, 53-59.

[44] Speirs, M., Dadbakhsh, S., Buls, S., Kruth, J. P., Van Humbeeck, J., Schrooten, J., & Luyten, J. (2013, September). The effect of SLM parameters on geometrical characteristics of open porous NiTi scaffolds. In *High Value Manufacturing: Advanced Research in Virtual and Rapid Prototyping: Proceedings of the 6th International Conference on Advanced Research in Virtual and Rapid Prototyping, Leiria, Portugal, 1-5 October.*

[45] Hamilton, R. F., Palmer, T. A., & Bimber, B. A. (2015). Spatial characterization of the thermal-induced phase transformation throughout as-deposited additive manufactured NiTi bulk builds. *Scripta Materialia, 101*, 56-59.

[46] Krishna, B. V., Bose, S., & Bandyopadhyay, A. (2007). Laser processing of net-shape NiTi shape memory alloy. *Metallurgical and Materials transactions A, 38*(5), 1096-1103.

[47] Halani, P. R., Kaya, I., Shin, Y. C., & Karaca, H. E. (2013). Phase transformation characteristics and mechanical characterization of nitinol synthesized by laser direct deposition. *Materials Science and Engineering: A, 559*, 836-843.

[48] Malukhin, K., & Ehmann, K. (2006). Material characterization of NiTi based memory alloys fabricated by the laser direct metal deposition process. *Journal of Manufacturing Science and Engineering, 128*(3), 691-696.

[49] Bormann, T., Müller, B., Schinhammer, M., Kessler, A., Thalmann, P., & de Wild, M. (2014). Microstructure of selective laser melted nickel–titanium. *Materials characterization, 94*, 189-202.

[50] Kalidindi, S. R. (2015). *Hierarchical materials informatics: novel analytics for materials data*. Elsevier.

[51] Louthan Jr, M. R., Caskey Jr, G. R., Donovan, J. A., & Rawl Jr, D. E. (1972). Hydrogen embrittlement of metals. *Materials Science and Engineering*, *10*, 357-368.

[52] Hansen, N. (2004). Hall–Petch relation and boundary strengthening. *Scripta Materialia*, *51*(8), 801-806.

[53] Thompson, M. K., Moroni, G., Vaneker, T., Fadel, G., Campbell, R. I., Gibson, I., & Martina, F. (2016). Design for Additive Manufacturing: Trends, opportunities, considerations, and constraints. *CIRP annals*, *65*(2), 737-760.

[54] Rickenbacher, L., Spierings, A., & Wegener, K. (2013). An integrated cost-model for selective laser melting (SLM). *Rapid Prototyping Journal*, *19*(3), 208-214.